UNIVERSITY OF MOLISE

Dept. of Medicine and Health Sciences "V. Tiberio"

PhD course in TRANSLATIONAL AND CLINICAL MEDICINE
XXX CYCLE

S.S.D Area-05 - Bio 10 Biochimica
S.S.D Area-05 - Bio 14 Farmacologia

DOCTORAL THESIS

STUDY ON PROTEASES INVOLVEMENT IN DUAL PROCESSING OF LOW-DENSITY LIPOPROTEIN RECEPTOR-RELATED PROTEIN 8 IN ALZHEIMER'S DISEASE

Tutor:
Prof. Claudio RUSSO

PhD Student:
Alessandro MEDORO
Matr. 153749

Coordinator:
Prof. Ciro COSTAGLIOLA

Academic year: 2016/2017

INDEX

INTRODUCTION

Alzheimer's Disease: clinical features, genetic and staging

Alzheimer's disease (AD) is a multifactorial condition and represents the most common form of senile dementia. The prevalence rate of AD was estimated about 35% in the population over 85 y.o. [1].

According to the estimates done by the World Alzheimer Report 2016, nowadays, about 47 million people worldwide suffer from a form of dementia and AD contributes to about 60%. This scenario is destined to double every 20 years, reaching about 131 million people affected in 2050, partly due to the increase of population longevity, partly to the increasing knowledge about clinical manifestations and pathophysiological processes in AD. Notoriously, in AD, dementia is characterized by the impairment of episodic memory, but the mere presence of this symptom does not confirm the diagnosis of the disease; similarly, the absence, at the beginning, of the memory involvement does not exclude AD diagnosis. In fact, other clinical manifestations include depression, apathy, agitation, disinhibition, hallucinations, aggression.

In the International Classification of Diseases (ICD-10), dementia is defined as "a syndrome caused by a chronic or progressive brain disease, in which a disorder of higher cortical functions is present, including memory, thought, orientation, comprehension, calculation, learning ability, language and judgment. Consciousness is not blurred. The impairment of cognitive functions is usually accompanied, and occasionally preceded, by deterioration of emotional control, social behaviour or motivation".

In the Diagnostic and Statistical Manual of Mental Disorders (DSM-5, 2013) the term "dementia" is replaced by "major neurocognitive disorder", characterized by a significant cognitive decline, compared to a previous level of performance, in attention, executive skills (planning, decision, working memory, problem solving, etc.), learning and memory (immediate memory, recall memory), language (expression and comprehension), perceptual abilities (visual and constructive), social

cognition. These deficits interfere with the independence and the abilities of patients daily activities [2].

Concerning the diagnosis, since 1907, when the first Alzheimer's patient was described [3], the main pathological hypothesis was related to macroscopic changes in the brain of affected patients compared to the unaffected ones: nowadays, non-invasive exams, such as computed tomography and nuclear magnetic resonance, show a progressive diffuse cortical atrophy and dilatation of the lateral ventricles, especially in advanced stages of pathology.

The NINCDS-ADRDA Alzheimer's criteria, proposed in 1984 by the "National Institute of Neurological and Communicative Disorders and Stroke" and the Alzheimer's Disease and Related Disorders Association (today Alzheimer's Association) are yet the most used in the diagnosis of AD and are based on neuropsychological testing for a clinical diagnosis of possible or probable AD on the basis of the presence of cognitive impairment and a suspected dementia; the definitive diagnosis is based on the histopathologic confirmation [4]. The Consortium to Establish a Registry for Alzheimer's Disease (CERAD) uses also clinical and histopathologic findings to establish the diagnosis of AD [5].

The main neuropathological changes are generally found in hippocampus, temporal cortex and Meynert nucleus: amyloid β (Aβ) plaques and intracellular neurofibrillary tangles (NFT) are the typical microscopic findings. According to the "amyloid hypothesis" Aβ derives from the cleavage by β- and γ-secretases of the amyloid precursor protein (APP), a transmembrane glycoprotein encoded in the chromosome 21. Aβ peptides, in their oligomeric and monomeric isoforms, are responsible of neurodegeneration, and of the accumulations of helix-wrapped neurofilaments in the cytoplasm of neurons, formed by iper-phosphorylated Tau protein (NFT). Other important alterations found in AD include oxidative stress, mitochondrial dysfunction, inflammation, neuron degeneration.

Anatomopathological signs correspond to the clinical evolution, as suggested by Braak and Braak (B&B) classification, which proposes six stages of AD. In the

transentorinal phase (stages I and II), the signs of the pathology are essentially confined to the entorhinal and transentorinal cortex, with low hippocampus involvement. The limbic phase (stages III and IV) is characterized by the presence of the NFT in the entorhinal cortex, with progressive and moderate involvement of hippocampus, amygdala, thalamus and hypothalamus. At last, the neocortical phase (stage V and VI) is characterized by the progressive involvement of neocortex (**Figure 1**) [6,7].

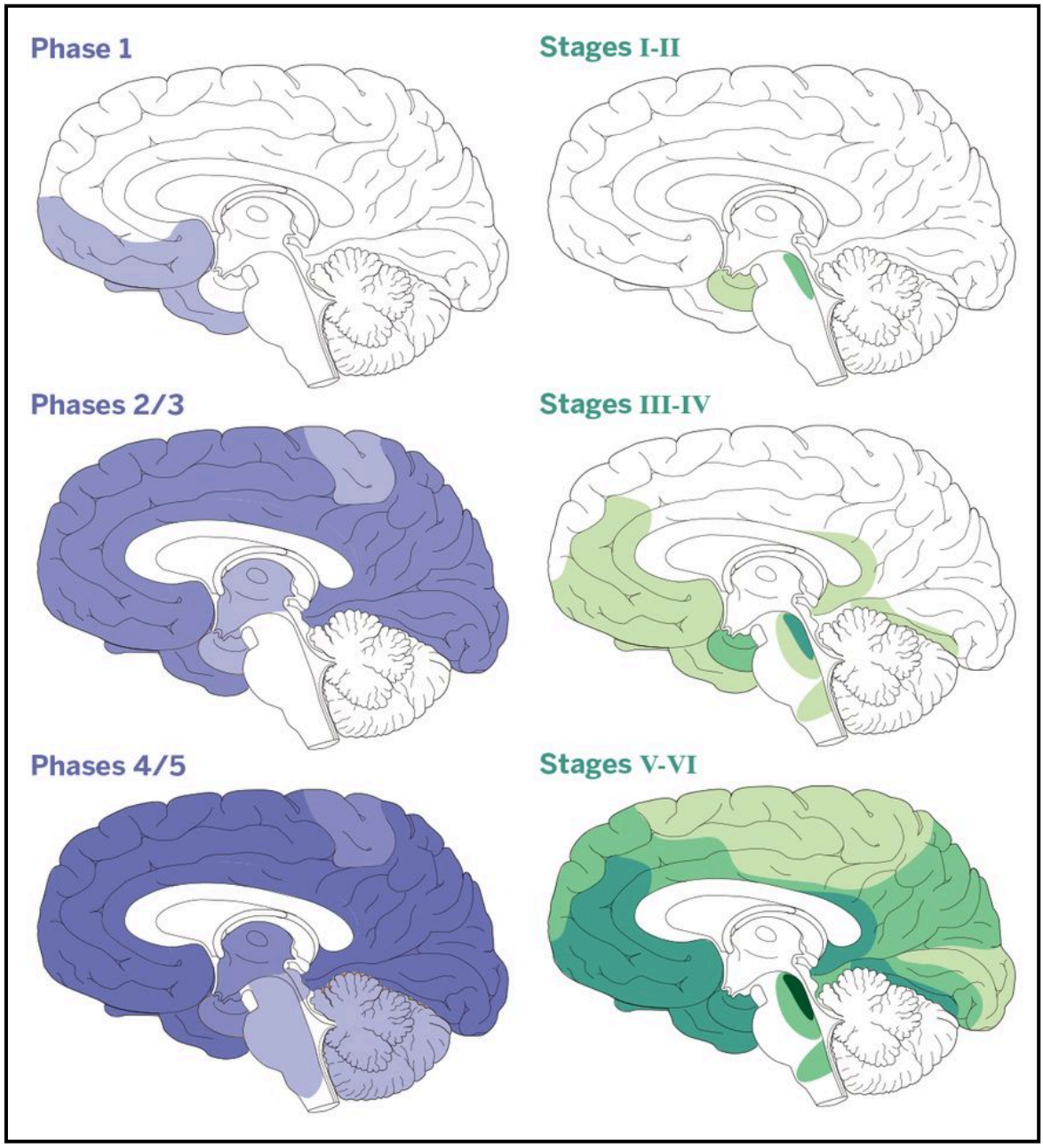

Figure 1 – Propagation of Aβ (blue) and Tau (green) in human brain during AD (adapted from Goedert, 2015). (Blue) Firstly, Aβ plaques are present in the basal temporal and orbitofrontal neocortex (phase 1). They are observed later throughout the neocortex, in hippocampus, amygdala, diencephalon, and basal ganglia (phases 2 and 3). In severe cases of AD (late stages), Aβ plaques are also found in mesencephalon, lower brainstem, and cerebellar cortex (phases 4 and 5). (Green) NFT develop in the locus coeruleus, in the transentorhinal and entorhinal regions (stages I and II). Subsequently, Tau inclusions are present in hippocampal formation and some regions of the neocortex (stages III and IV), followed by almost all neocortex (stages V and VI).

Finally, in the terminal stages, AD patient becomes unable to walk, incontinent, dysphagic, can present neuromuscular rigidity and other extrapyramidal signs and symptoms. The average survival is about 10 years from the diagnosis; death generally occurs due to intercurrent diseases, such as urinary or respiratory infections.

There are different forms of AD, based on genetics and age of clinical onset: familial early-onset form (FAD), that begins in subjects between 30 and 50 years old, and the sporadic forms: late-onset (SAD), after 65 years old, and early onset SAD, before 65 y.o. FAD has a genetic basis, in fact, it has been associated with mutations of three genes, APP on chromosome 21 (this gene was the first discovered), Presenilin 1 (*PSEN-1*) on chromosome 14 and Presenilin 2 (*PSEN-2*) on chromosome 1: both are often reported as presenilins (PSENs), the functional subunits of γ-secretase, an enzyme responsible of the processing of APP.

On the other hand, SAD is the most frequent form of AD and represents about the 98% of cases. The etiology of SAD is still not completely understood: probably, it is a combination of environmental factors and genetic predisposition. Great importance in the onset of both forms is played by the Apolipoprotein E (*ApoE*) gene, that is the main component of lipoproteins, responsible of carrying lipids, such as cholesterol, in the blood and other body fluids, and the most studied risk factor in AD. In particular, the allele e4, which is present in 10-20% of the population, has a strong association

with AD, anticipating the onset of the disease and increasing the risk of developing AD three times in heterozygous individuals and ten times in homozygous ones [8].

Diagnosis of AD is difficult and largely dependent on cognitive and functional assessments, due to the absence of a clinical marker useful to identify the disease during the first phase of the onset. At present, definite diagnosis is possible only in post-mortem analysis of the brain and upon neuropathological assessment of plaques, NFT and other microscopic typical signs such as local inflammation and astrogliosis, amyloid angiopathy, Lewy bodies etc... Despite the great efforts of research in the field, up-to-date there is no cure for AD and the current treatment options are considered to be symptomatic. These therapies being essentially based on the modulation of acetylcholine or glutamate neurotransmitters, through acetylcholinesterase inhibitors or N-methyl-D-aspartic acid (NMDA) antagonist, respectively. In Europe, the costs for dementias are estimated to € 106 billion per year [9].

Amyloidogenic hypothesis: APP and γ-secretase

As mentioned above, APP is central in AD pathogenesis. It is a type I transmembrane receptor and belongs to a family that include APL-1 in *C. elegans*, APPL *in Drosophila* and APP-like protein 1 (APLP1) and 2 (APLP2) in mammals. APP shares several conserved domains with these two last receptors, including the E1 and E2 domains in the extracellular sequences and the intracellular domain; not the Aβ domain, that is a unique motif in APP. APP functions are not well-defined, although a role in neurite outgrowth and synaptogenesis, neuronal protein trafficking along the axon, transmembrane signal transduction, cell adhesion, etc. has been proposed [10].

APP gene is located on chromosome 21 and alternatively spliced isoforms of this gene are reported with different length ranging from 305 to 770 aminoacids. Among these, splicing isoforms are differently expressed in human brain: e.g. isoform 695 is expressed and predominant in neurons [11], while isoforms 751 and 770 are mainly expressed in astrocytes [12].

Full-length APP is sequentially processed by at least three proteases that are named α-, β- and γ-secretases Cleavage in the APP extracellular side by α-secretases (several zinc metalloproteases, as TACE/ADAM17, ADAM9, ADAM10 and MDC-9) or β-secretase (the neuronal enzyme is mainly an aspartyl-protease, termed BACE1 or memapsin 2) produces soluble fragments of the receptor (named APPsα and APPsβ, respectively) [13–15].

The membrane-bound C-terminal fragments produced by β-secretase are known as C99 and C89 and are then processed by γ-secretase: a high molecular weight protein complex, with specific “intramembrane-cleaving aspartyl-protease activity” (I-CLiPs) or, also, “regulated intramembrane proteolysis” (RIP) [16,17]. γ-secretase cleavage leads to the liberation of the amyloid intracellular domain (AICD), with a yet unclear transcriptional role at nuclear level [18] and to a family of soluble amyloid β-peptides (Aβ), which are released as monomers or oligomers into the lumen. The α-secretase cleavage-site is located within the Aβ domain, producing a 3 kDa product,

named p3, and a membrane-bound fragment (C59); precluding the generation of Aβ, this pathway is called “nonamyloidogenic” (**Figure 2** [19]).

Processing of APP by β- and γ-secretases is considered a pivotal event in the genesis of AD: according to the “amyloid hypothesis”, the soluble forms of Aβ initiate and contribute to AD pathogenesis [20,21]. In fact, the “amyloid hypothesis” states that the aberrant processing of APP by γ-secretase induces the formation of specific neurotoxic soluble Aβ peptides - mainly those isoforms ending at residue 42 ($A\beta_{42}$), in respect to the $A\beta_{40}$, which, in turn, cause neurodegeneration [22]. The amyloid hypothesis, according to which the formation of soluble, oligomeric Aβ peptides in the brain is the primary influence driving AD [23,24], is, at present, the dominant model of AD pathogenesis.

In this theory the role of ApoE as AD risk factor is crucial. Although circulating ApoE is produced and secreted primarily by the liver, in the brain it is synthesized mainly by astrocytes and microglia cells to provide cholesterol to neurons, where it is essential to create and maintain the neuronal plasticity. In humans there are three main allelic variants of the *ApoE* gene (ε2, ε3, ε4), which code 3 protein isoforms (ApoE2, ApoE3, ApoE4) of 299 amino acids, which differ only in two residues: E2 (C112, C158), E3 (C112, R158), E4 (R112, R158), but with different biological properties.

ApoE4 appears to be less efficient than the two other isoforms in cholesterol uptake and in promoting its transport between astrocytes and neurons. These data suggest that the differences among ApoE isoforms could influence the pathogenesis of AD acting on cholesterol homeostasis [25]. Furthermore, ApoE is also involved in the binding and clearance of Aβ, toward which ApoE3 and ApoE2 have a higher affinity compared to ApoE4 [26,27].

In vivo studies showed that knockout ApoE mice, crossed with AD mice overexpressing APP, exhibit less Aβ deposition, compared to those expressing ApoE3 or ApoE4. These studies show that ApoE regulates the deposition of Aβ and that ApoE4 can increase the risk of AD, favouring amyloid deposition levels [28,29].

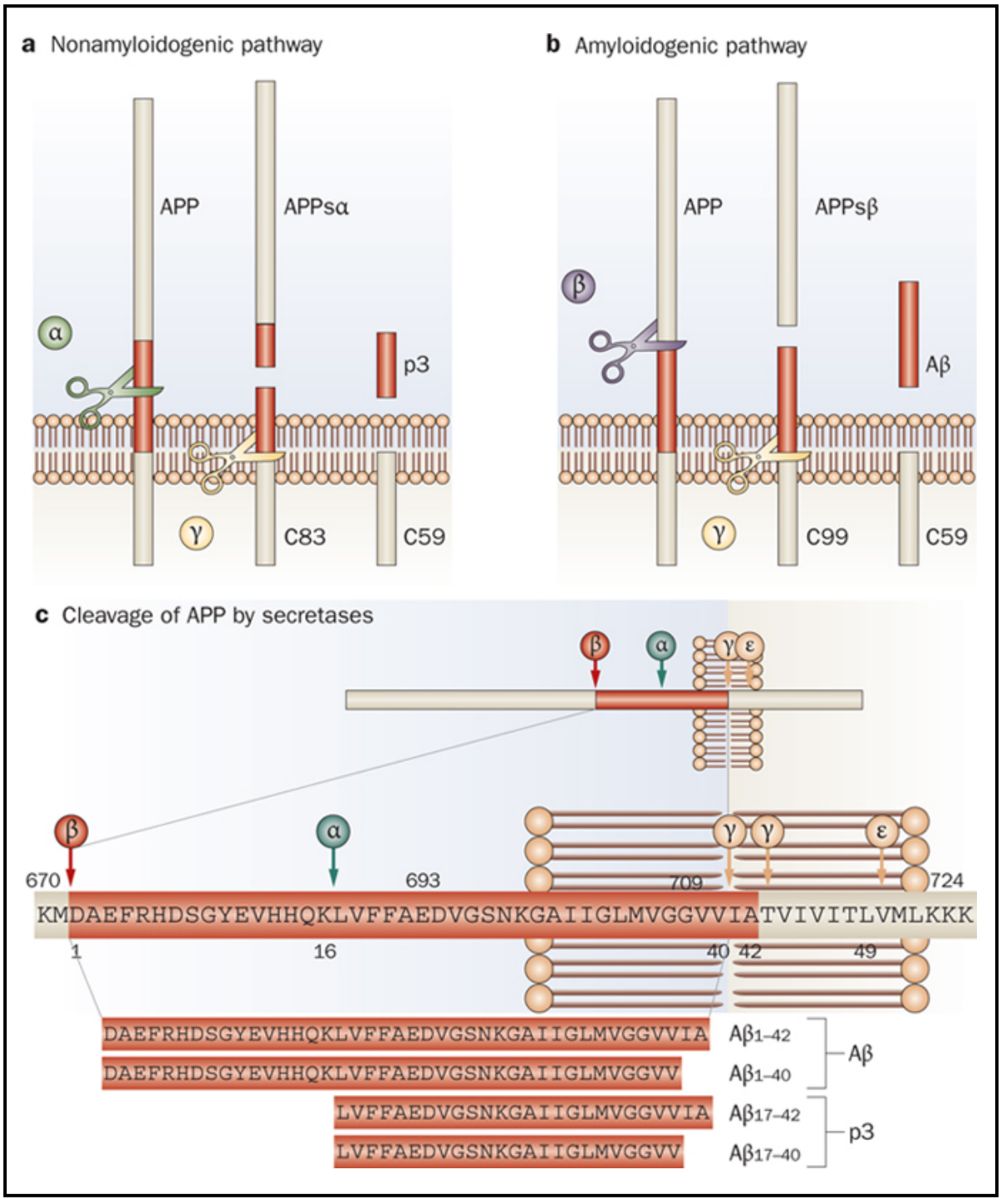

Figure 2 – Schematic view of nonamyloidogenic (A) and amyloidogenic (B) pathways. (C) Detail of secretases cleavage on APP sequence. Adapted from De Strooper et al., 2010.

The γ-secretase complex is made by four transmembrane proteins (**Figure 3** [30]): heterodimeric PSENs (either PSEN-1 or PSEN-2 which are 65% identical), nicastrin (NCT), the anterior pharynx-defective 1 (APH-1) and the presenilin enhancer 2 (PEN-2) [31]. NCT, a glycosylated 130 kDa type I protein, is principally involved in substrate recognition and selectivity [32]; APH-1 (there are two isoforms, APH-1A and APH-1B) regulates γ-secretase activity and position of cleavage site on APP [33]; PEN-2 is functionally required for endoproteolysis and for stabilization of the most important components: PSENs, which represent the catalytic core of the γ-secretase complex [31,34].

PSENs are synthesized as full-length proteins, but their structure seems to be unstable and are quickly either endoproteolysed or degraded. This intramolecular autocatalytic event, that induces a cleavage between residues N292 and V293 on PSEN-1, is required for γ-secretase activation upon formation of a stable heterodimer between the amino-terminal fragment (NTF ~30 kDa, transmembrane domain, TMD, 1-6) and the carboxyl-terminal fragments (CTF ~20 kDa, TMD 7-9) [35,36]. The intramolecular arrangement of TMD 6 and TMD 7 represent the biologically active structure of this protein, bearing in close proximity the two aspartic acids (D257 and D385 residues), which are essential for the PSENs catalytic activity [37].

APP is the most studied γ-secretase substrate, however, the list of putative substrates includes more than 90 proteins [38]. Most of them are type-I transmembrane cell surface adhesion molecules, and receptors with a cytoplasmic C-terminus often involved in the initiation and mediation of intracellular signalling such as: cell differentiation, adhesion, migration, neurite outgrowth, axon guidance, or formation and maintenance of synapses [38].

Among different γ-secretase substrates, some can directly interact with APP: as Alcadein α/Calsyntenin-1, Deleted in Colorectal Cancer, LDL Receptor family, Notch and p75-neurotrophin receptor [39].

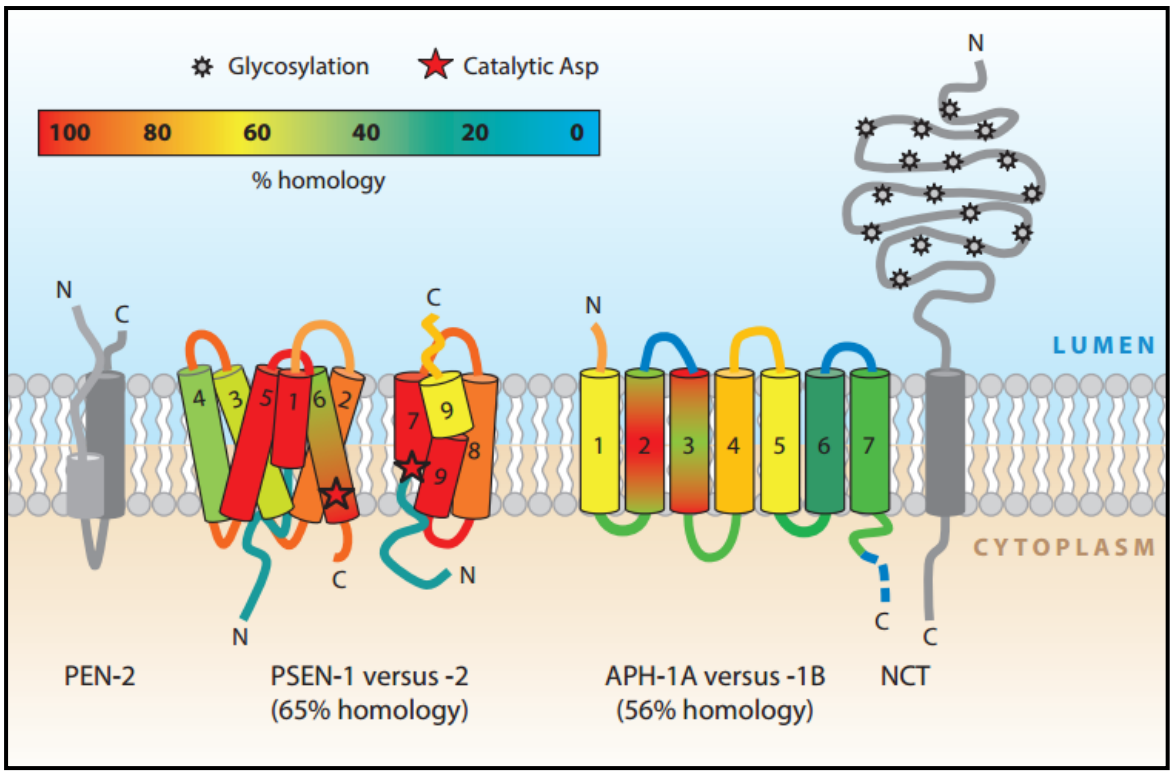

Figure 3 – Schematic structure of γ-secretase (adapted from De Strooper and Gutierrez, 2014). Colours in the scale indicates the level of sequence homology between PSEN-1 and PSEN-2 and APH-1A and APH-1B.

During searches for genes responsible for early-onset FAD [40,41], *PSEN* genes were the first identified (subsequently, mutations on *APP* gene were identified). Currently over than 220 AD-causing mutations have been identified and most of them are localized on *PSEN-1* gene (chromosome 14), while only a minor group are located on *PSEN-2* gene (chromosome 1), as reported in Alzforum database (www.alzforum.org/mutations) [42]. Pathogenic PSENs mutants cause an increment of soluble $A\beta_{42}$ in respect to $A\beta_{40}$ [43], that is considered central and pivotal in AD genesis. Emerging experimental evidences suggest that the loss of essential functions of PSENs could better explain dementia and neurodegeneration in AD [44,45]: conditional inactivation of PSENs in the adult mouse brain causes progressive memory loss and neurodegeneration resembling AD [46,47]. In view of these results, a new theory emerged claiming that PSENs mutants may be more likely related to a "loss-of-function" on γ-secretase, than to a "gain-of-function".

Whether this may have an influence on $A\beta_{42}/A\beta_{40}$ ratio (or vs. other substrates of γ-secretase), it is yet unclear [39].

However, familial patients with very early onset and bearing specific *PSEN-1* mutations have also a peculiar brain pattern of soluble $A\beta_{42}$, characterized by increasing amounts of N-terminal truncated and pyroglutamate-modified peptides, such as AβN3pE-42 and AβN11pE-42 in comparison to SAD cases [48]. These shortened peptides are more neurotoxic and more prone to oligomeric assembly than $A\beta_{40/42}$ peptides [49].

The second most commonly involved gene is *APP*, with 27 pathogenic mutations described in Alzforum database. In APP, mutations cluster around the γ-secretase cleavage site (French, German, London, Indiana, Florida, etc.), although the most famous APP mutation (Swedish, APP-sw) causes a change in amino acids adjacent to the BACE1 cleavage site.

Other AD pathogenetic hypothesis

Tau hypothesis

The Tau hypothesis claims that the ultimate cause of the neurodegeneration is an excessive or abnormal hyper-phosphorylation of Tau, which determines the Tau protein transformation into PHF-Tau (paired helical filament) and then into NFT. Tau is a highly soluble protein that interacts with tubulin to stabilize the cytoskeleton microtubules. There are six different Tau isoforms, with different and peculiar length: the longest one is formed by 441 aminoacids, has four repetitions (R1, R2, R3 and R4) and two inserts, and is located in CNS, while the shorter form has three repetitions (R1, R3 and R4) and no insert (352 total amino acids). In AD conditions, all adult brain isoforms are in a hyper-phosphorylated state. The process of Tau aggregation, without genetic mutations is not clear: it may be due to an abnormal equilibrium between kinases and phosphatases [50]. Tauopathies are referred as a class of neuropathological conditions characterized by neurodegeneration and NFT, in which dementia, often familial, it is linked to mutations on Tau and to NFT (in absence of plaques) [51,52]. Hyperphosphorylated Tau dissociates from microtubules and sequestrates normal Tau proteins to form NFT. This insoluble structure damages cytoplasmic functions and interferes with axonal transport, which can lead to cell-death [53]. The open question in AD is: besides Aβ, which are the conditions that lead to NFT formation in absence of Tau mutations?

Inflammation hypothesis

Increasing evidence suggests that inflammation plays a crucial role in the early stages of AD: microglia, astrocytes and neurons are involved in the complex neuroinflammatory process. The Aβ peptides can activate microglia, with an increased expression of the major histocompatibility complex II (MHC II) on the cell surface, of pro-inflammatory cytokines, such as IL-1β, IL-6, TNFα, IL -8, MIP-1 α and of chemotactic proteins for monocytes [54]. Aβ also induces a phagocytic response in microglia and the expression of nitric oxide synthase (NOS) with consequent neuronal damage [51].

Astrocytes can cluster Aβ deposits and secrete interleukins, prostaglandins, leukotrienes, tromboxanes, coagulation factors and protease inhibitors. Neurons are also able to express significantly higher levels of pro-inflammatory molecules and molecules involved in the complement cascade [55].

ROS hypothesis

Reactive oxygen species (ROS or free radicals), which mainly coming from the mitochondrial electron transport chain (ETC), can mediate cellular oxidative damage and cell death [56]. Oxidative phosphorylation is the first source of free radicals, such as hydrogen peroxide (H_2O_2), hydroxyl radical (OH) and superoxide radical (O_{2-}). Oxidative damage affects lipids, proteins, nucleic acids and sugars, all organic compounds essential for the structural and functional integrity of neurons.

In AD an inhibition of ETC is observed, with accumulation of electrons in complex I and in coenzyme Q, which can be directly donated to oxygen molecules forming the superoxide radical which, then, reacts with nitric oxide, making the radical peroxynitrite ($OONO^-$). The AD is also characterized by an antioxidant capacity deficiency, in fact there is a reduction of the activity of the enzyme Cu/Zn superoxide dismutase (SOD) and a deficiency of glutathione (GSH). In these conditions free radicals can produce cell damage without being countered by antioxidants [57].
ROS also have two other effects: mediating DNA oxidation, with double helix breakage, protein cross-linking and modifications of the nitrogenous bases; glico-oxidation with consequent accumulation of AGEs (advanced glycation end-product) that can produce more ROS, leading to further advancement of AD.

Cell cycle hypothesis

The cell cycle hypothesis proposes that mitogenic signalling and/or cell cycle control are altered in brain neurons of patients with AD: high expression levels of proteins implicated in regulation of the cell cycle are found (CDKs, cyclin-dependent kinase). Adult brain neurons are definitively differentiated cells, still in the G0 phase and without the possibility of dividing, so the re-activation of the cell cycle can determine

a death signal. Nevertheless, there is no evidence of a real mitotic process, although these neurons probably stop at the step that precedes the event of cell division [58]. The cell receives the starting signal and the expression of A cyclin marks a no return-point. The cell cannot go back in G0 phase but can only go on completing the cycle or dying.

Because of there is no evidence of conclusion of a mitotic division, the cell-death option is considered more possible than others. Several in vivo studies, in which powerful oncogenes have been expressed in neurons, show that cells are able to replicate their DNA (beginning of the cell cycle), but subsequently undergo cell death [59].

The activation of the cell cycle is related to the development of NFT. In fact, in addition to regulating the cell cycle, CDKs are implicated in Tau phosphorylation, as showed in different *in vitro* and *in vivo* studies. Moreover, CDKs expression precedes the appearance of hyperphosphorylated Tau, indicating a cause-effect connection [60].

Furthermore, highly phosphorylated Tau is found in the mitotically active cells during the brain development phase. On one side, *in vitro* experiments have shown that APP is involved in the activation of the cascade, in particular in the activation of proteins that regulate the cell-cycle; on the other side, *in vivo* it has been seen that even the modest over-expression of APP in neurons, in which this protein is mutated (FAD), leads to DNA synthesis and neuronal apoptosis [61].

γ-secretase inhibitors

In the last years, a crucial hub for neural processes and the principal target for AD therapeutics is the intricate γ-secretase complex; representing one of the most intensely protease ever investigated [62], harboring ~90% of all identified mutations causative of FAD in its catalytic components: the PSENs. PSENs are essential components for embryonic development: PSEN-$1^{-/-}$ mice die at birth, while PSEN-$1/2^{-/-}$ mice die during early embryonic stage [63].

Due to its central role in APP processing and amyloid formation, the γ-secretase complex is a preferential drug target in AD therapy. In the last years, many clinical trials were carried out using γ-secretase inhibitors or modulators, although with disappointing results. The most striking case is the one of Semagacestat (LY450139) trial of Eli Lilly [64–66]: a promising γ-secretase inhibitor able to reduce Aβ formation *in vitro* experiments and in the brain, cerebrospinal fluid, and plasma in animal models [67]. Clinical tests were prematurely stopped because of severe side effects as skin cancer, infections and weight loss. However, the principal unexpected effect induced by chronic treatment with γ-secretase inhibitor was the worsening of the cognitive abilities of treated patients.

The unexpected short inductions of complete γ-secretase inhibition, used in these clinical trials, might have critical effects on other biochemical pathways, involved in oscillating systems, such as Notch signalling oscillations, implicated in memory processes. After all, severe Notch phenotypes have already been observed after the complete γ-secretase inactivation in mice models [47,68–70] and it was clear that blocking Notch signalling were severely limiting the clinical use of Semagacestat (LY450139) [71].

Furthermore, neither evidences about the possible different affinities between γ-secretase components and their substrates are available, nor the mechanisms of the cleavage induced by γ-secretase are still clear. Indeed, other γ-secretase inhibitors, including Avagacestat, also turned out to be far less selective for APP than vs. Notch processing [65,72], paving the way to the use of γ-secretase inhibitors in cancers

treatment with promising results in various cancer types: in fact, Notch signalling plays key roles in carcinogenesis and cancer progression, in particular in the establishment of mesenchymal phenotype during cancer progression and metastasis [73].

Besides all these aspects, therapeutic approaches based on inhibition of γ-secretase catalytic activity, has clashed with real-world negative results; likely due to the poor and unclear information about the structure and function of γ-secretase, the significant number of substrates cleaved, and the physiological significance of their γ-secretase-mediated processing in different cell types.

A link between APP, ApoE and γ-secretase: Low-density Lipoprotein Receptor-Related Protein 8 (LRP8)

The LDL receptor family is an apparently homogeneous group of cell surface receptors involved in a wide range of cellular signalling pathways [74]. Most of these receptors are processed through iCliPS by γ-secretase (after sheddase activity), some of which interact with APP: Very Low-Density Lipoprotein Receptor (VLDLR), Low-Density Lipoprotein Receptor-related Protein 1 (LRP1), Low-Density Lipoprotein Receptor-Related Protein 8 (LRP8), Sortilin-related receptor 1 (SorL1) and Sortilin (Sor). They share with APP common cytosolic signalling adaptors such as FE65, X11/Mint and Disabled-1 (Dab1), and they are all receptors for ApoE [74]. The mechanisms by which ApoE influences AD onset and development is still unclear and, there are two opposite hypotheses prevailing: either ApoE, in its various isoforms, is involved in complexes with Aβ whose relative stability affects their toxicity or clearance [75–77]; or ApoE outcomes descend from different and parallel biological processes, in which the family of LDL receptors plays a predominant role [78–81].

Among the receptors of this family, LRP8, or Apolipoprotein E Receptor 2 (ApoER2) has a crucial role in this context. LRP8 immunoreactivity in human hippocampus was identified only in neurons and in fine granular structure of reactive astrocytes surrounding amyloid plaque in APP-sw mice [82].

Some LDL receptors may modulate, at the same time, formation and vascular clearance of Aβ, where LRP1 principally modulates this function [83–86], synaptic plasticity and dendritic spine formation [87], or may control neuronal migration and formation of cortical layers [88,89]. The latter feature is triggered by Reelin, which is a soluble ligand of LRP8, *via* phosphorylation of the adaptor Dab1 [90], that binds the cytosolic portion of APP: in detail, Reelin facilitates the interaction of LRP8 and APP with Dab1 and, in parallel, triggers the processing of both receptors by γ-secretase [91]. More recently, LRP8 was described as crucial in the control of multiple processes in neuronal migration, including the early stage of radial migration and termination of migration beneath the marginal zone in the developing neocortex [92].

Mice lacking functional Reelin, LRP8 or Dab1 presents the same phenotypes: cortical, hippocampal and cerebellar neurons fail to migrate properly during development [93,94]. The same phenotype is observed in APP KO models [95,96]. LRP8 is also receptor of F-spondin, a component of the extracellular matrix involved in neuronal migration and plasticity in adult and developmental brain: this binding is able to affect the APP processing, resulting in decreased production of Aβ [97,98].

This APP-LRP8 interaction seems to be also involved in the increase of cell surface APP levels (because the increase of cell surface APP requires the presence of LRP8 cytoplasmic domain) resulting in the decreased APP internalization rate. Interestingly, LRP8 expression correlates with a significant increase in Aβ production and reduced levels of APP-CTFs. The increased Aβ production was dependent on the integrity of the NPXY endocytosis motif of LRP8: expression of LRP8 increases APP association with lipid rafts and γ-secretase activity, both of which might contribute to increased Aβ production [86].

The crosstalk between LDL receptors and APP is even more complex if we look at another common cytoplasmic interactor: in fact LRP1, LRP8 and VLDLR bind to FE65, a cytoplasmic adapter protein, forming different tripartite complexes [99] which may modulate APP endocytic trafficking, Aβ production, AICD nuclear trafficking and DNA protection [100–102]. It is worth to remember that, if on one side AICD, along with FE65 and Tip60/Kat5, associates into complexes in nuclear transcription factories, on the other one also the C-terminal portions of LDL receptors are recruited at nuclear level upon γ-secretase cleavage [103,104]. At the same time, AICD along with FE65 and Tip60/Kat5 block LRP1 transcription [105], suggesting that APP proteolytic processing by γ-secretase reduces LRP1 brain levels possibly hampering both Aβ clearance and Reelin signalling.

Apparently, NMDA receptors are also conditioned by Reelin and LDL receptors which recruit Dab1 and facilitate Ca^{2+} entry through NMDA channels [74]. In general, ApoE receptors are synaptic proteins that affect the activity of glutamate receptors in the post-synaptic density modulating long-term potentiation, memory and learning. In this

context PSD-95, an adaptor protein directly involved in the post-synaptic density, interacts with LRP8, through the alternatively spliced intracellular exon, and with NMDA receptors [106,107]. Interestingly, the alteration of Reelin/LRP8/PSD-95 by the expression of a mutant LRP8 (LRP8-tailless), which is unable to interact with PSD-95, hampers Reelin signalling (robust dendritogenesis in mature hippocampal neurons *in vitro*) [108].

This activity is needed for learning and memory function: the Reelin-LRP8 pathway is required for hippocampal-dependent associative learning and is involved in the epigenomic modifications required for memory formation. In fact, LRP8-KO mice show a severe impairment in freezing behaviours that reflects a loss of long-term memory formation [104]. In detail, the proteolytic processing of LRP8 with the release of LRP8 intracellular domain (ICD), which seems to translate into the nucleus, represents a synapse-to-nucleus communication promoted by Reelin: apparently, this activity needed for learning and memory function is negatively regulated by ApoE4 and arises from the regulated proteolysis of LRP8 or LRP1 by γ-secretase [79,104,109]. Interestingly, LRP8-ICD is a negative regulator of Reelin, thus suggesting a feedback regulatory system triggered by γ-secretase cleavage of LRP8 [110]. However, as far as neuronal migration concerns, Reelin signalling is apparently intact in PSEN-1$^{-/-}$ primary neuronal cultures, where γ-secretase activity is not required for Reelin-induced phosphorylation of Dab1 [111].

Interestingly, PSEN-1 mutations show impaired γ-secretase activity relatively to LRP8, and an accumulation of its C-terminal fragments, both products of sheddase and γ-secretase, after Reelin exposure: this last effect is potentiated by co-exposure to DAPT, a γ-secretase inhibitor [112].

AIMS OF THE STUDY

The “amyloid hypothesis”, has recently evidenced significant limitations and, in particular, the following issues are debated:

1) the concept and significance of PSEN “gain-of-function” vs. “loss-of-function” [44,45];
2) the presence of several and various proteins as substrates of γ-secretase, which interact with APP and may influence Aβ formation [38].

The latter consideration is suggestive: despite the increasing number of γ-secretase substrates so far identified, their reciprocal interaction with APP itself, even in the AD field, is significantly unexplored.

We decided to investigate a new hypothesis: the possibility that APP is co-processed by γ-secretase with a second receptor and that a putative “loss-of-function” of γ-secretase would affect the second receptor, rather than APP, thereafter, inducing neurodegeneration and hampering its signalling/activity.

Among almost 90 different substrates of γ-secretase, we focus our attention on LRP8, which has the following features:

1) it is an APP interactor;
2) it is expressed at neuronal level;
3) it is a receptor of ApoE, which is the most important risk factor for developing AD;
4) it is, at least in theory, involved in signalling activities compatible with neuronal migration or cell proliferation and memory processes [86,91,104,112–115].

Finally, its α-elical transmembrane region is very similar to that of APP, and the putative consensus site (V V - I A) for the cleavage by γ-secretase in that region is almost identical, while LRP1 shows significant differences.

Therefore, in this thesis we will explore the processing of LRP8 in human brain, in human cerebrospinal fluid and plasma and *in vitro* cell culture systems, to ascertain its theoretical linkage with AD - either in sporadic or familial forms -, to verify its

putative dependence on APP and on γ-secretase, or on other proteolytic enzymes potentially involved in AD genesis.

MATERIALS AND METHODS

Human brain and cerebrospinal fluid samples

Cerebral cortex and cerebellum were obtained by autopsy from clinically and neuropathologically verified (based on CERAD criteria and B&B classification) cases of sporadic late onset AD (SAD, total n. 17, average age 75,20±13,80 y.o.), of familial early-onset AD (FAD, total n. 6, average age 45,70±6,65) and aged non-demented control subjects (total n. 21, average age 77,00±10,30 y.o.), in which AD has been excluded by clinical, autopsy examination and immunohistochemical analysis, as described in **Table 1**.

Frozen brain samples were collected at autopsy and derive from the Brain Bank of Case Western Reserve University, Cleveland, OH, USA, from the Joseph and Kathleen Bryan Alzheimer's Disease Research Center (Bryan ADRC) at Duke University Medical Center, Durham, NC, USA and from the Human Brain and Spinal Fluid Resource Center at University of California, Los Angeles, CA, USA. Three small pieces of grey matter from frontal and temporal cortices and cerebellum were excised under sterile conditions and collected as a unique sample representative of each brain areas [116].

Table 1 – Demographic and clinical information about patients analyzed. + to +++ symbols indicate the crescent quantity of amyloid plaques. N.A.= not available; Neg.=negative.

	ID number	Mental Status	Sex	Age	Amyloid plaques	Notes
1	3484	Normal	M	72	+	Normal
2	4294	Normal	M	80	Neg.	Normal
3	4307	Normal	M	84	Neg.	Aging
4	4308	Normal	M	70	Neg.	Aging

5	3216	Normal	M	79	Neg.	B&B III
6	3482	Normal	F	79	Neg.	Normal
7	4514	Normal	M	66	Neg.	Normal
8	4593	Normal	M	76	Neg.	Aging
9	4621	Normal	F	83	Neg.	Normal
10	4660	Normal	F	73	Neg.	Normal
11	4956	Normal	F	92	Neg.	Normal
12	4320	Normal	M	87	Neg.	Aging
13	O94-35	Normal	F	49	Neg.	Normal
14	A94-122	Normal	N.A.	82	Neg.	Infarct
15	4332	Normal	M	63	Neg.	Normal
16	3298	Normal	M	79	Neg.	Hypoxia
17	963	Normal	F	82	+	B&B III
18	3482	Normal	F	79	Neg.	Normal
19	984	Normal	F	65	+	B&B I
20	1169	Normal	M	88	Neg.	Normal
21	787	Normal	F	90	+	B&B I
34	A_96-296	SAD	N.A.	82	+++	B&B IV
33	A97-9	SAD	N.A.	89	++	B&B III
22	3219	SAD	F	88	++	B&B III

23	3233	SAD	F	78	+++	B&B V
36	3244	SAD	F	79	+++	B&B VI
24	3268	SAD	F	89	++	B&B II
35	3270	SAD	F	60	+++	B&B VI
25	3278	SAD	F	81	++	B&B III
32	3285	SAD	F	61	++	B&B III
26	3288	SAD	F	41	++	Early-onset, B&B III
38	3291	SAD	F	55	+++	B&B V
27	3301	SAD	F	80	++	B&B III
28	3316	SAD	F	77	++	B&B V
29	3327	SAD	M	88	++	B&B IV
30	3329	SAD	F	74	+++	B&B VI
31	4091	SAD	F	88	+	B&B I
37	4098	SAD	F	68	+++	B&B V
39	124	FAD	M	40	+++	B&B V
40	178	FAD	M	44	+++	B&B V
41	313	FAD	F	48	+++	B&B IV
42	734	FAD	M	41	+++	B&B V
43	967	FAD	F	43	+++	B&B VI
44	1024	FAD	F	58	+++	B&B V

All FAD patients have mutations on *PSEN-1* gene: 178, 313 and 1024 have H163R mutation, 734 and 967 have M139I mutation, while 124 has M146L mutation. All these mutations are reported as pathogenic in Online Mendelian Inheritance in Man (OMIM) database.

We had also the opportunity to analyze 11 samples of post-mortem ventricular cerebrospinal fluid: 4 control non-demented subjects, 4 SAD and 3 FAD patients.

Human plasma samples

Blood collection (in collaboration with Prof. Di Costanzo from University of Molise) was done between 8:00 and 8:30 a.m. after an overnight fasting of at least 12 h. Venous blood was collected into Vacutainer serum tubes (Becton & Dickinson, Italy) and centrifuged within 4 h. All serum samples were stored at −80°C.

As already described [117], patients with amnestic mild cognitive impairment (MCI), that is defined as impairment of 1 or more cognitive domains that is worse than expected for the age and level of education of an individual, but is not severe enough to significantly compromise daily activities, met the National Institute on Aging-Alzheimer's Association (NIA-AA) criteria [118] for MCI due to AD [119] had Mini-Mental State Examination scores >24 and Clinical Dementia Rating scores of 0.5, and showed memory impairment as assessed via age/sex/education-adjusted scores on at least 1 of the following tests: Rey's word list, immediate and delayed recall, and prose memory, immediate and delayed [120].

In total 21 patients were analyzed, 10 cognitively healthy (average age 73,7±2,62) and 11 MCI subjects (average age 68,60±8,65), as reported in **Table 2**. All patient samples were analyzed in triplicate.

Table 2 – Demographic and clinical information about patients of which plasma samples were analyzed

	ID number	Mental Status	Sex	Age
1	48	Control	F	77
2	56	Control	F	76
3	58	Control	M	76
4	65	Control	F	73
5	68	Control	M	72
6	69	Control	F	70
7	109	Control	M	72
8	175	Control	F	76
9	301	Control	M	75
10	317	Control	F	70
11	8	MCI	F	70
12	15	MCI	M	75
13	17	MCI	M	81
14	24	MCI	F	73
15	33	MCI	F	71
16	64	MCI	M	64
17	73	MCI	M	62
18	77	MCI	F	70
19	135	MCI	M	76
20	181	MCI	F	49

21	205	MCI	M	64

RNA extraction from brain samples

RNAs were extracted from cerebral samples using PureLink RNA Mini Kit (Life Technologies, USA), according to the manufacturer's instructions. Fresh lysis buffer (0,6 ml per 30 mg of tissue) was prepared adding 2-mercaptoethanol (10 µl for each 1 ml lysis buffer) to the sample, before homogenization, which was performed using a rotor-stator homogenizer at maximum speed for >45 seconds. The lysate was centrifuged at 26,000 x g for 5 minutes, 70% ethanol was added to each volume of cell homogenate, and each sample was transferred to the spin cartridge for washing steps. Finally, RNA was eluted using DNAse and RNAse free water.

The quality of extracted RNA was evaluated by measuring 260/280 nm optical density using NanoDrop 2000 (Thermo Fisher, USA).

cDNA synthesis

1 µg of total RNA was reverse-transcribed using High capacity cDNA Reverse Transcription kit (Applied Biosystems, USA), according to manufacturer's instructions. The reaction was performed using Mastercycler thermal cycler (Eppendorf, Germany) under standard amplification conditions up to 40 amplification cycles: briefly, a reaction master mix was assembled and added to each RNA sample, along with sufficient RNAse-free water, for a final volume of 20 µl, followed by incubation in a thermal cycler at 25°C for 10 minutes, 37°C for 120 minutes, 85°C for 5 minutes, and hold at 4°C. The cDNA samples were tested for gDNA contamination: the overall level of which was ≤0.05%

Real Time-PCR

FAM-MGB Taqman assays were purchased from Applied Biosystems, USA. Genes, accession numbers, probes localization are given in **Table 3**. From 1 to 10 are listed

the target genes, included *EIF4A2* [121] and *GAPDH* that were chosen as endogenous control genes.

Real time-PCR experiments were performed using ABI Prism 7900HT platform (Applied Biosystems, USA). Briefly, each sample was run in triplicate in each experimental set and the amplification mix contained 1X TaqMan Assay, 1X TaqMan Master mix and roughly 100 ng of cDNA for a final volume of 10 µl under standard amplification conditions up to 45 amplification cycles [122]. Data collection was set at the annealing/extension step (60°C). Primary analysis was done within the SDS 2.3 data collection software (Applied Biosystems, USA). Secondary analysis was done for up to 10 plates at time within the Relative Quantification Manager 1.2 (Applied Biosystems, USA). Differentially expressed genes were assessed by means of the ΔΔCt algorithm [123], using the total human brain RNA (Catalog #:AM6050, Applied Biosystems, USA) as calibrator sample which underwent to the same cDNA synthesis and amplification procedures.

Table 3 – TaqMan gene expression assays

	Gene Name	Assay ID	Accession numbers	Exon-exon boundaries	Amplicon length (bp)
1	*ADAM10*	Hs00153853_m1	NM_001110.3	11-12	83
2	*ADAM17*	Hs01041915_m1	NM_003183.5	13-14	54
3	*ADAMTS1*	Hs00199608_m1	NM_006988.4	1-2	68
4	*CTSD*	Hs00157205_m1	NM_001909.4	5-6	103
5	*CTSL*	Hs00964650_m1	NM_001257971.1	5-6	87
6	*EIF4A2*	Hs00756996_g1	NM_001967.3	3-4	133
7	*GAPDH*	Hs99999905_m1	NM_001289746.1	2-2	122

8	*MEP1A*	Hs00194410_m1	NM_005588.2	13-14	75
9	*MEP1B*	Hs00195535_m1	NM_001308171.1	9-10	102
10	*MMP9*	Hs00234579_m1	NM_004994.2	12-13	54

Cell cultures and transient transfection with Lipofectamine 3000

N2A cells (a mouse neuroblastoma immortalized cell line) wild-type (wt) or stably transfected with the plasmid encoding for hHA-LRP8 and MEF cells (mouse embryonic fibroblast) wt or PSEN-1/2 KO were grown in plastic Petri dishes (100 mm or 60 mm, according to the different experimental procedure) in DMEM (Dulbecco's Minimum Eagle Medium) supplemented with 10% Fetal Bovine Serum (FBS) decomplemented at 56°C for 30 minutes, 1% L-glutamine (2 mM in 0.85% NaCl), 1% penicillin (50 U/L) and streptomycin (50 µg/mL) in a humidified atmosphere at 37°C with 5% CO_2: all these products were purchased from Gibco, USA. hHA-LRP8 N2A cells were cultured with additional G418 (Sigma, USA) to maintain cells that express the plasmid the hHA-LRP8. N2A and MEF cells were transiently transfected with hLRP8-ddk-myc, hLRP8 C-terminus (C-Term LRP8) or EGFP using Lipofectamine 3000 (Thermo Fisher Scientific, USA), according to the manufacturer's protocol.

Drugs

BMS708163, LY450139, YO01027 were purchased from Selleckchem, Germany, DAPT and NU-9056 from Tocris Bioscience, UK and ALLN from Merck-Millipore, USA. All the drugs were dissolved in dimethyl sulfoxide (DMSO). In the experiments performed *in vitro*, drugs were added to culture medium for 16 h incubation.

SDS-PAGE and Western Blots experiments

Western Blot (WB) experiments were performed using human brain, plasma and ventricular cerebrospinal fluids samples and cell lysates:

- Brain samples were homogenized with RIPA Buffer 1x in a ratio 1:4, that is composed by 500 mM Tris pH 7.6, 50 mM EDTA, 5% sodium deoxycholate, 1% SDS, 10% NP40, complemented with protease inhibitors 1x, sodium orthovanadate 1 mM (Na3VO4), sodium fluoride 10 mM (NaF) and phenylmethanesulfonyl fluoride 1 mM (PMSF), in a rotor-stator homogenizer at maximum speed for 30 seconds, then were centrifuged at 20,000 x g for 20 minutes at 4°C and supernatants were collected, as described in literature [48].
- Plasma and ventricular cerebrospinal fluids samples were centrifuged at 14,000 x g for 10 minutes at 4°C and supernatants were collected. Plasma samples were diluted 1:5 in Milli-Q water to improve the electrophoresis separation.
- Cell culture were washed three times with Phosphate-Buffered Saline (PBS) and lysed with RIPA Buffer 1x. The samples were collected with scrapers and incubated for 30 minutes in ice, then where centrifuged at 14,000 x g for 15 minutes and supernatants were collected.

Samples protein amount was determined using Bradford (Bio-Rad, Italy) and all these samples were then loaded with Sample Buffer 2x (SDS 8%, glycerol 24%, Tris 100 mM, tricine 100 mM, dithiothreitol 15 mg, Coomassie brilliant blue g-250 0.05%) in a Tris-Tricine SDS PolyAcrylamide Gel Electrophoresis (SDS–PAGE), with different % of acrylamide according to the experimental needs and transferred to a PVDF membrane 0.22 µm (Amersham, UK). Membranes were blocked by an incubation of 2 h in Phosphate-buffered saline Tween-20 (PBS-T) containing 5% non-fat dried milk and blotted over night with the appropriate primary antibodies: rabbit polyclonal anti-LRP8 (named GS1, GeneScript, USA), rabbit polyclonal anti- C-terminus of APP (Zymed, Zymed Laboratories, USA), mouse monoclonal anti-ADAMTS1 (LS-C339246, LifeSpan BioSciences, USA); mouse monoclonal anti-Cathepsin D (D-7 sc-377299, Santa Cruz, USA); rabbit polyclonal anti-Meprin (ab204886, Abcam, UK), mouse monoclonal anti-γ tubulin (GTU-88, Sigma-Aldrich, USA). After washing with PBS-T, the membranes were incubated with opportune peroxidase-conjugated secondary antibodies for 1 h at room temperature. After washing the reactive bands were revealed with ECL Plus Western Blotting Detection

Reagents (Amersham, UK). In some experiments, PVDF membranes were stripped to remove the primary antibody used by incubation for 30 minutes in the stripping solution (glycine 0.2 M, SDS 20%, Tween20, pH 2.2) and then for 10 minutes in PBS-T. The PVDF membranes were successively blocked and incubated with a different primary antibody. All images were acquired by an automated gel imaging instrument, Gel Doc EZ System (Bio-Rad, Italy). Densitometric analysis of protein bands was performed using ImageLab software system (Bio-Rad, Italy).

Immunohistochemistry and Immunocytochemistry experiments

Immunohistochemistry (IHC) experiments were performed on paraffin-embedded cerebral slices of patients reported in the **Table 1**. The protocol used is the following:

- formalin-fixed, paraffin-embedded slices were deparaffinised in 100% xylene (Sigma, USA) for 2 times for 5 minutes;
- they were then transferred to 100% alcohol (Carlo Erba, Italy) for 5 minutes, to 80% alcohol for 5 minutes and rinsed in distilled water for two times for 5 minutes;
- antigen retrieval to unmask the antigenic epitopes were performed using citrate buffer method: slices were arranged in a staining container with 10 mM sodium citrate buffer, pH 6.0 and incubated at 95-100°C for 2 minutes and then removed to room temperature (RT) for 2 minutes; this step was repeated for 4 times;
- the staining container were removed to RT and the slices were allowed to cool for 15 minutes and then were washed for 2 times with PBS 1x and incubated with PSB+0,3% Triton for 10 minutes at RT;
- slices were washed in PBS 1x for 5 minutes and incubated with blocking solution (PBS 1x + 10% Normal Goat Serum, NGS, Sigma, USA) for 45 minutes;
- slices were incubated with primary antibodies (rabbit polyclonal anti-LRP8, named GS1, GeneScript, USA and mouse monoclonal anti-phosphorylated TAU, AT100, Sigma, USA over night at 4°C;
- slices were washed for 3 times with PBS 1x for 5 minutes and then incubated with a solution (PBS 1x + 10% NGS) with secondary antibodies

(anti-rabbit red Alexa Fluor® 568 and anti-mouse green Alexa Fluor® 488, ThermoFisher, USA) and DAPI (Sigma, USA) for 1 hour at RT;

- slices were washed for 3 times with PBS 1x for 5 minutes and then incubated with Sudan Black solution (70% Ethanol + 0.3% Sudan Black, Sigma, USA) to block the autofluorescence, a natural emission of light by some biological structures;
- slices were washed for 3 times with PSB 1x for 5 minutes and then were cover slipped using Mowiol (Sigma, USA) mounting solution over night at RT;

Immunocytochemistry (ICC) experiments were performed as following:

- cells were culture on 12 mm round glass slips and transiently transfected as described above;
- cell culture medium was removed and cultured cells were fixed with cold 4% paraformaldehyde for 15 minutes;
- cell cultures were washed 3 times with PBS 1x for 3 minutes, 2 times with PBS 1x + 0,1 M glycine (Sigma, USA) for 5 minutes and again 3 times with PBS 1x for 3 minutes;
- cell cultures were incubated with Blocking solution (PBS 1x + 10% NGS, Sigma, USA) for 20 minutes, then with primary antibody for 40-45 minutes (rabbit polyclonal anti-LRP8, named GS1, GeneScript, USA) and washed with PBS 1x 3 times for 3 minutes and then 1 time for 5 minutes;
- cell cultures were incubated with a solution (PBS 1x + 10% NGS) with secondary antibody (anti-rabbit red Alexa Fluor® 568, ThermoFisher, USA) and DAPI (Sigma, USA); then they were washed with PBS 1x 3 times for 3 minutes and then 1 time for 5 minutes and then cover slipped using Mowiol (Sigmaa, USA) mounting solution over night at RT;

All IHC and ICC images were obtained using Eclipse inverted fluorescence microscope (Nikon, Japan).

Statistical analysis

Data are reported as mean value ± standard error of the mean (SEM), and statistical significance was examined using the unpaired Student's t-test, with the threshold set at $p<0.05$ (*=$p<0.05$;**=$p<0.01$;***=$p<0.001$,****=$p<0.0001$) or the ANOVA test-Tukey's multiple comparisons test with the threshold set at $p<0.05$ (*=$p<0.05$;**=$p<0.01$;***=$p<0.001$,****=$p<0.0001$), C.I. 95%, to evaluate the statistical significance in the analysis of more than two different groups. All the analyses were performed using GraphPad Prism (v.7; GraphPad Software, USA).

RESULTS

PART I

A specific C-terminal-recognizing antibody to study the processing of LRP8

Human LRP8 (hLRP8) protein (Uniprot Q14114) has 4 main different splicing isoforms: isoform 1 (LRP8-963), isoform 2 (LRP8-700), isoform 3 (LRP8-904) and isoform 4 (LRP8-793). Here is the alignment of the C-terminal region of each isoform (**Figure 4**).

```
Q14114   LRP8_HUMAN   781   TAAVPSSVSVPRAPSISPSTLSPATSNHSQHYANEDSKMGSTVTAAVIGIIVPIVVIALL   840
Q14114-2 LRP8_HUMAN   610   --------------------------------NEDSKMGSTVTAAVIGIIVPIVVIALL   636
Q14114-3 LRP8_HUMAN   781   TAAVPSSVSVPRAPSISPSTLSPATSNHSQHYANEDSKMGSTVTAAVIGIIVPIVVIALL   840
Q14114-4 LRP8_HUMAN   611   TAAVPSSVSVPRAPSISPSTLSPATSNHSQHYANEDSKMGSTVTAAVIGIIVPIVVIALL   670
                                                  ***************************

Q14114   LRP8_HUMAN   841   CMSGYLIWRNWKRKNTKSMNFDNPVYRKTTEEEDEDELHIGRTAQIGHVYPAAISSFDRP   900
Q14114-2 LRP8_HUMAN   637   CMSGYLIWRNWKRKNTKSMNFDNPVYRKTTEEEDEDELHIGRTAQIGHVYPARVALSLE-   695
Q14114-3 LRP8_HUMAN   841   CMSGYLIWRNWKRKNTKSMNFDNPVYRKTTEEEDEDELHIGRTAQIGHVYPARVALSLE-   899
Q14114-4 LRP8_HUMAN   671   CMSGYLIWRNWKRKNTKSMNFDNPVYRKTTEEEDEDELHIGRTAQIGHVYPAAISSFDRP   730
                            ************************************************ ::   .

Q14114   LRP8_HUMAN   901   LWAEPCLGETREPEDPAPALKELFVLPGEPRSQLHQLPKNPLSELPVVKSKRVALSLEDD   960
Q14114-2 LRP8_HUMAN   696   ------------------------------------------------------DD   697
Q14114-3 LRP8_HUMAN   900   ------------------------------------------------------DD   901
Q14114-4 LRP8_HUMAN   731   LWAEPCLGETREPEDPAPALKELFVLPGEPRSQLHQLPKNPLSELPVVKSKRVALSLEDD   790
                                                                              **

Q14114   LRP8_HUMAN   961   GLP                                                       963
Q14114-2 LRP8_HUMAN   698   GLP                                                       700
Q14114-3 LRP8_HUMAN   902   GLP                                                       904
Q14114-4 LRP8_HUMAN   791   GLP                                                       793
                            ***
```

Figure 4 – Alignment of proximal N-terminal, transmembrane and C-terminal regions of the 4 isoforms of human LRP8: exon 18 is conserved only in isoform 1 (900-958 aa) and 4 (730-788 aa).

LRP8 isoform 1 is the longest and was used in our *in vitro* studies using cDNAs expressing the wt form tagged at the C-terminus with ddk-myc or at the N-terminus with HA. The transmembrane region V I G I I V P I V V I A L L C M S G Y L I is conserved in all isoforms. The putative cleavage by γ-secretase is at the V V – I A site, which is identical to the APP site that forms Aβ-40 (**Figure 5**). All isoforms contain the D N P V Y motif (similar to that of APP) necessary for internalization and interaction with adaptor proteins.

The sequence A I S S F D R P L W A E P C L G E T R E P E D P A P A L K E L F V L P G E P R S Q L H Q L P K N P L S E L P V V K S K which is present only in

isoforms 1 and 4, is determined by exon 18 in humans. Its presence is typical of mammalian and is apparently linked to memory processes and Reelin activity [104].

Initially, to study the LRP8 proteolytic processing in human, we designed a polyclonal antibody targeted to a specific C-terminal region of the protein, using the following sequence as immunogen: C - D E D E L H I G R T A Q I G (C has been added to couple the peptide to KLH). This sequence is present in all 4 major splicing isoforms; it consist of a short sequence with charged aminoacids and it is located between the N P X Y (D N P V Y in LRP8) motif and the exon18 sequence. The corresponding antibody is called GS1.

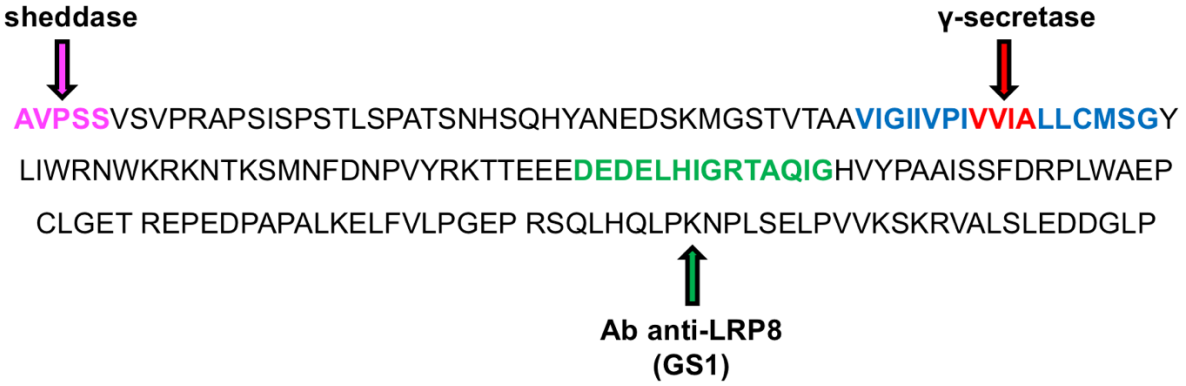

Figure 5 – Schematic view of proximal N-terminal, transmembrane and C-terminal regions of the LRP8 isoform 1: fuchsia sequence is the processing site of sheddase (a yet unclear cleavage likely exerted by furin-like protease), blue region is the LRP8 transmembrane region, red sequence represents the proteolytic site of γ-secretase and green region is the sequence used as immunogen to produce our antibody anti-LRP8 (GS1).

Ex vivo analysis in human brain of LRP8 processing in SAD and FAD vs. control subjects: reduction of full-length LRP8 and enhancement of LICDs in AD vs. non-AD brains

In a first instance, we analyzed the protein levels of LRP8 in human brain samples (frozen frontal and temporal cortices) from SAD (n=10, average age 72,40 y.o.) and

control non-demented (n=11, average age 79,20 y.o.) subjects by Tris-Tricine SDS-PAGE followed by Western blotting (as described in *Material and Methods*). We also analyzed different brain areas (frontal cortex, temporal cortex and cerebellum) in a group of FAD subjects (n=6, average age 45,00 y.o.) carrying PSEN-1 mutations (*see Materials and Methods*). Non-demented controls and SAD patients are age-matched, to avoid possible differences in LRP8 expression and/or processing linked exclusively to the age. However, due to the early onset of FAD, age-matching is not possible.

WB experiments show that in SAD and FAD brain areas analyzed there is a marked presence of C-terminal fragments of LRP8 intracellular domains (LICDs), ranging from 8 to 12 kDa, detected by the GS1 antibody. Interestingly, these low molecular weight (MW) fragments are never described in the literature, to-date. In parallel, we observe a significant decrease of the full-length proteins (FL) migrating at 105 kDa, as described in a representative WB experiments in **Figure 6**. Bands migrating at around 100-105 kDa represent different human LRP8 isoforms and/or post-translational modifications on each isoform (upper panel in **Figure 6**).

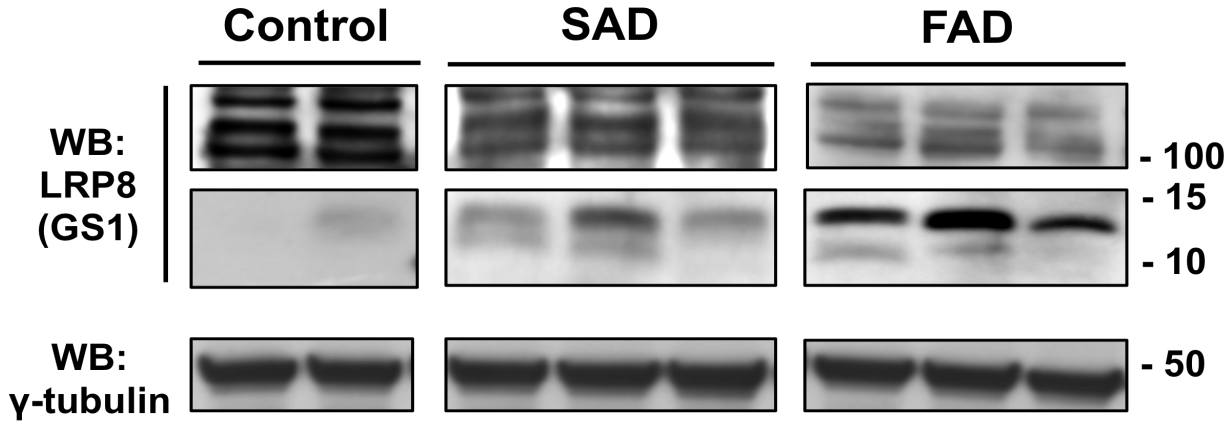

Figure 6 - Representative WB of *ex vivo* brain LRP8 processing. 2 cases of control non-demented, 3 SAD cases and 3 FAD cases revealed an evident reduction of FL and a significant increase in LICDs in SAD and FAD patients compared to the control non-demented subjects in frontal and temporal cortices. Cerebellum of FAD patients were also analyzed.

Considering only the FL protein levels, a decrease in FAD patients is evident, with a parallel increment of LICDs. SAD patients showed an intermediate behaviour. The increased presence of LICDs indicate a likely augmented processing of LRP8 promoted by γ-secretase activity.

To verify these features, we performed densitometric analysis by informatics tools (ImageLab) of LRP8 bands identified by GS1 antibody in each group, using as housekeeping reference protein the highly stable γ-tubulin. Total LRP8 expression (summarizing LRP8 FL and LICDs fragments) is not statistically significant (**Figure 7 A**) among groups; the value of each samples analyzed in these experiments was normalized in comparison to the average value of the control group: the total LRP8 expression is 1,00±0,20 in the control non-AD subjects, 0,90±0,24 in the SAD patients 1,39±0,16 in FAD subjects.

On the other side, If we extend the analysis comparing the ratio of LRP8 FL/LICDs in our subjects, we can appreciate the important and significant reduction of FL protein and the parallel increment of LICDs in FAD and SAD cases, in comparison to non-demented subjects (**Figure 7 B**). In detail, the control non-AD group has a LRP8 FL/LICDs ratio of 1,01±0,18, while the SAD group has a marked and statistically significant ($p<0,0001$) increase of LICDs with a ratio of 4,82±0,92, compared to the control group.

In FAD cases, the difference is even more pronounced and in some patients we observed more than 80 times LICDs than in controls (*not shown*). On average the ratio of LRP8 FL/LICDs was 19,26±2,12 and is statistically significant with ANOVA test compared to the control non-demented subjects ($p<0,0001$), but not vs. SAD patients; likely because the reduced number of patients analyzed, although there is a significance with Student's t-test.

These data clearly indicate an altered processing of LRP8, but not an alteration in its cerebral expression, in familial and sporadic cases of AD compared to non-demented patients.

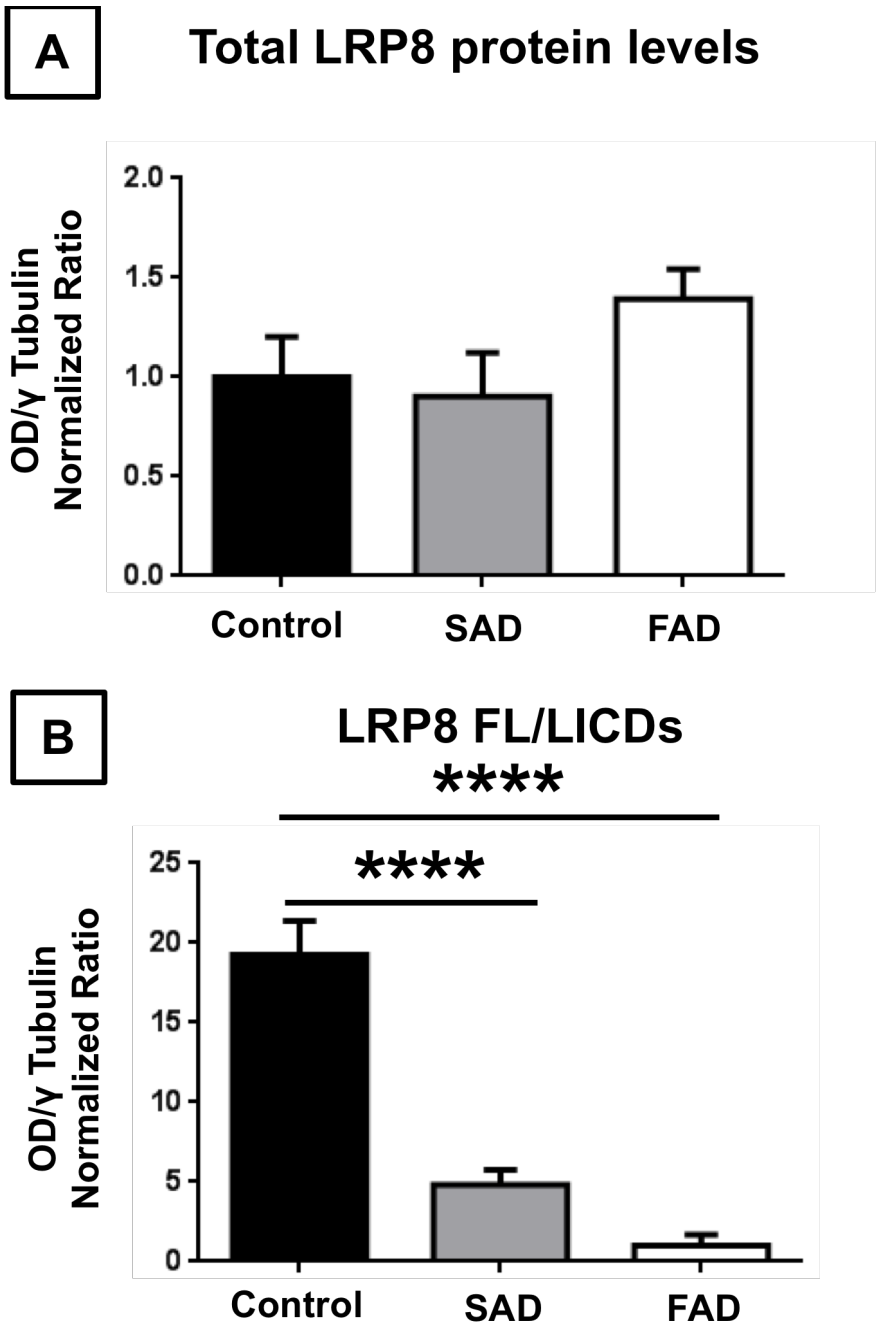

Figure 7 – Densitometric analysis of total LRP8 protein level (A) and of LRP8 FL/LICDs ratio (B) in control non-demented, SAD and FAD patients. (A) No significant differences are evidenced among the groups in the total LRP8 expression levels. (B) Densitometric analysis reveals a significant reduction of FL/LICDs ratio in SAD and FAD patients, that is statistically significant compared to the control non-demented subjects with ANOVA test analysis. No statistics significance are revealed with ANOVA test between SAD and FAD groups.

As described above, we had the opportunity to analyze LRP8, in selected FAD patients, also in cerebellar areas which in general are interested by the neuropathological features of AD only in the late stage of the disease, as in V-VI stages by Braak & Braak classification [6].

If we analyze FL/LICDs ratios in FAD samples only, and we extract the contribution of each cerebral area, measuring the average values of LRP8 FL/LICDs ratio in frontal cortex (n= 6), temporal cortex (n=6) and cerebellum (n=3) (normalized vs. γ-tubulin of each area) we observe that normalized value are: 1,05±0,36, 0,92±0,19 and 1,04±0,47, respectively (**Figure 8**). These data, indicate a likely altered LRP8 processing also in the cerebellum of the three FAD patients analyzed, who were at stage V by Braak & Braak. Further analysis in non-AD and SAD cerebellum are needed to accurately investigate this feature.

We can hypothesize, on the basis of these data, the possibility that the alteration of the LRP8 FL/LICDs ratio may be correlated to the severity of the disease; since FAD patients are characterized by very early onset, short duration and very severe dementia, while some subjects in the control group who are staged III by Braak & Braak and have plaques (as cases 3216 and 963) have normal LICDs levels and are clinically normal. Experiments on other control cases carrying plaques, and confronting different cerebral areas bearing plaques and NFT vs. non-bearing pathology in SAD or FAD patients, are needed to accurately investigate this feature.

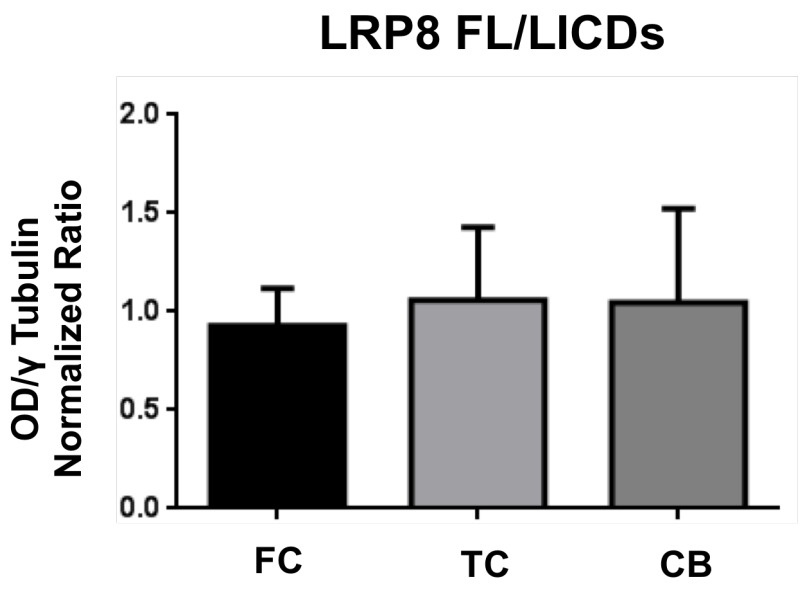

Figure 8 - Densitometric analysis of LRP8 FL/LICDs ratio of frontal cortex (FC), temporal cortex (TC) and cerebellum (CB) specimens from FAD patients. All data were normalized by housekeeping protein γ-tubulin. No differences are evidenced with ANOVA test.

Cerebral LRP8 distribution: AD vs. Control

We then performed IHC experiments on cerebral slices of the same subjects (non-demented, SAD and FAD subjects) and in the same brain areas analyzed (cortex) by WB, to study the distribution of LRP8. In **Figure 9**, we show a co-immunostaining with antibodies anti-LRP8 (GS1) and anti-phosphorylated Tau (pTau, AT100). The latter antibody recognizes two phosphorylated sites in the Tau protein (S212 and T214), which are present in pathological conditions in aggregated Tau as in NFT.

A specific LRP8-immunostaining distinguishes both SAD and FAD patients from non-demented controls. Keeping in mind that GS1 antibody does not discriminate between FL and LICDs, we observed a clear neuronal and intracellular staining (**Figure 9 A**) in control non-demented case, which is almost absent in SAD (**Figure 9 B**) and FAD (**Figure 9 C**) subjects, where, instead, we detected a diffuse parenchymal staining.

Indeed, in AD cases, as observed in merge figures (**Figure 9 B-C**), LRP8 maintains an intracellular and neuronal distribution only in the neurons that are not affected by NFT or Tauopathy, as indicated by the white arrows. No LRP8-staining is observed in the vasculature, confirming the data in the literature where only other members of the LRP family, as LRP1, are reported to be expressed in the vessels [124].

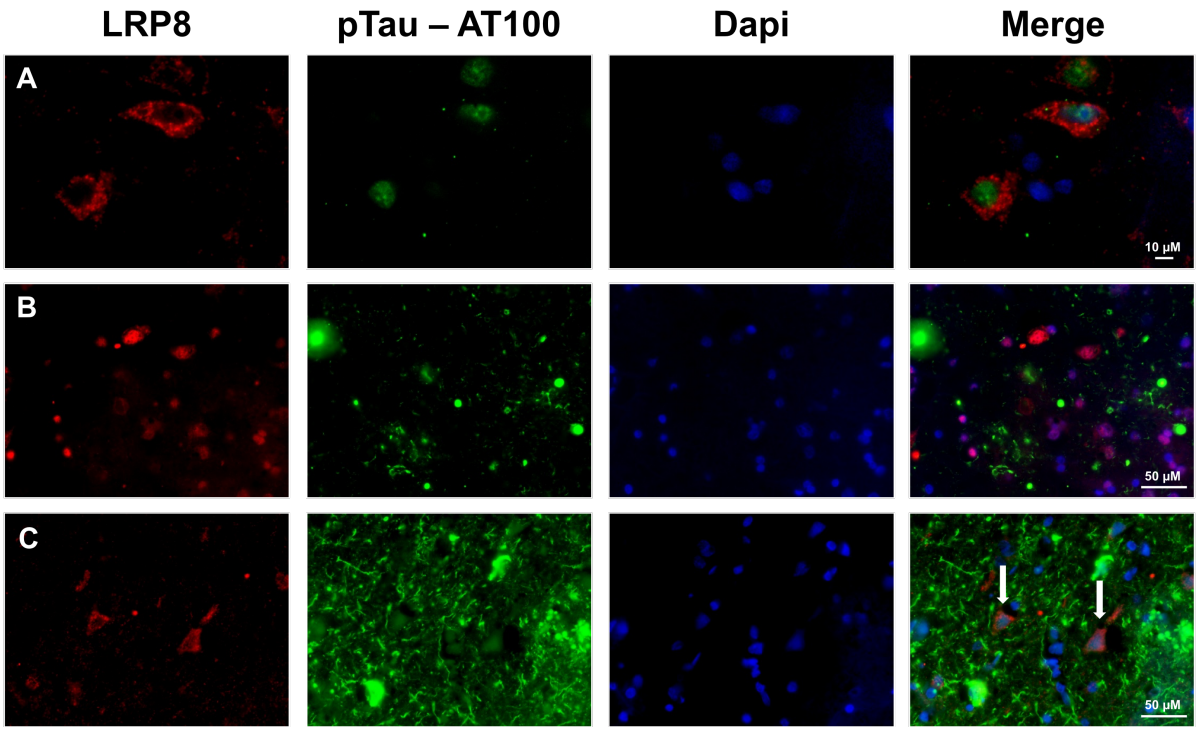

Figure 9 – IHC analysis of LRP8 (red), AT100 (green) and Dapi (blue, for nuclear staining) distribution in cerebral cortex of control non-demented (A), SAD (B) and FAD (C) subjects. The LRP8 staining is neuronal in the control group, while is parenchymal in AD subjects. White arrows indicate the neuron that are not affected by the presence of NFT or Tauopathy and where is maintained the neuronal staining of LRP8 in AD cases (B-C). Scale bars (µm) are reported in merge figures.

Analysis of LICDs peripheral pool in human plasma and cerebrospinal fluid

In parallel to brain samples, we processed plasma and liquor samples from AD and non-AD subjects, looking for the peripheral pool of LRP8. In particular, we had also the opportunity to analyze some samples from MCI subjects in which AD is in its earlier stage, to study whether the alteration of LRP8 processing could be useful as a marker in early phases.

We analyzed 11 samples of post-mortem ventricular cerebrospinal fluid of the same patients analyzed with WB and SDS-PAGE: 4 control non-demented subjects, 4 SAD and 3 FAD patients.

In **Figure 10**, it is shown a representative analysis by SDS-PGE and WB using the antibody GS1 of cerebrospinal fluids (post-mortem, ventricular samples) from control non-demented cases (lanes 1 and 4), a SAD case (lane 2) and from one familial case (lane 3), bearing a mutation on *PSEN-1*. The same protein amount was loaded for each sample. C-terminal fragments and LICDs (fragments between 10 and 15 kDa) are present only in AD cases (red box).

Green box evidences also the presence of LRP8 FL; because of the absence of a marker to normalize the values of the proteins of the samples, although the same quantities have been used, it is difficult to evaluate the quantitative significance related to their expression.

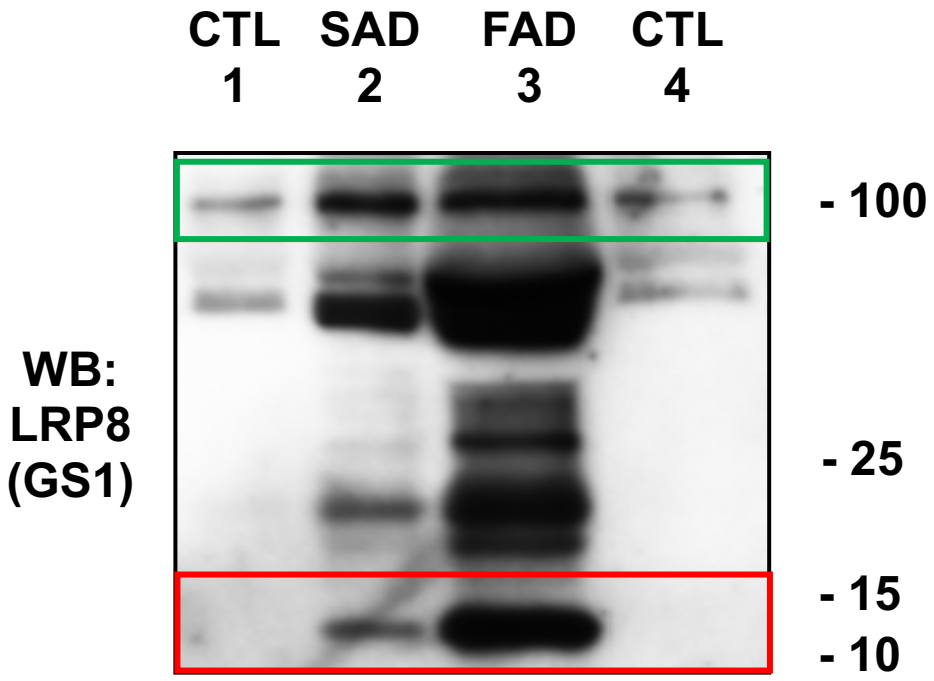

Figure 10 – Representative WB of post-mortem ventricular cerebrospinal fluid samples from control non-demented cases (1 and 4), a SAD case (2) and a FAD case (3). The lower band in AD samples migrates at ~12 kDa (red box) and is not present in control non-demented samples. Green box highlights LRP8 FL.

We also analyzed human plasma samples to verify the presence of LICDs pool also at peripheral level. The main problem concerning these samples being that we cannot be sure about the neat origin of LICDs fragments: whether they may derive from cerebrospinal fluid and brain or whether are they produced in other peripheral districts.

In WB experiments performed on human plasma samples, we detect a significant LICDs increment in MCI cases in respect of control subjects (**Figure 11**). In these experiments, however, information about LRP8 FL are not clearly interpretable because of the abundant presence of not specific signals due to the high content of proteins with an elevated MW (*not shown*).

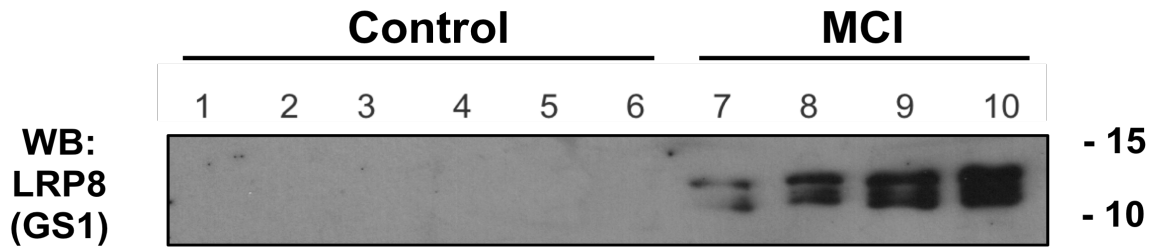

Figure 11 – Representative WB analysis of plasma samples from control (lanes 2-6) and MCI cases (7-10). This experiment shows peripheral LICDs presence only in MCI patients. Lane 1 contain the molecular marker. Antibody staining with GS1.

Both in ventricular cerebrospinal fluid and in plasma samples, the lower band detected with the antibody GS1 migrates at 12 kDa, as previously evidenced also in brain samples, suggesting that the altered LRP8 processing could be not limited only to the brain, but it could be found also at the periphery.

RESULTS

PART II

Inhibitors of γ-secretase, such as DAPT and BMS708163, increase LICDs in vitro model of N2A cells.

Previous reports evidenced that the C-terminal fragments of LRP8 (migrating between 25 and 20 kDa) are the substrate of γ-secretase activity that produce a fragment of about 15 kDa or about 18-19 kDa, as reported in literature [104,112]. Therefore, there are no reports describing shorter fragments under 15 kDa, likely because commercial antibodies are not able to distinguish such small fragments. On the contrary, in our studies, when we refer to LICDs we indicate only fragments migrating between 8-12 kDa. The hypothesis is, therefore, that these fragments are cleaved by γ-secretase, and the inhibition of γ-secretase would generate the accumulation of their precursors. We thus decided to use N2A (mouse neuroblastoma) cells, a common *in vitro* model of neuronal-like cell lines, stably transfected with human LRP8 bearing a N-terminal hemagglutinin tag (hHA-LRP8).

Cell cultures were treated with 4 different inhibitors of γ-secretase (BMS708163, LY450139, YO01027 and DAPT), or with PBS+0.1% DMSO (the same concentration of DMSO used to dissolve drugs) as control cells. All of them have IC50 in the nanomolar range either for APP or Notch processing. Some of them are used in clinical trial either to treat AD or cancer (as Notch processing inhibitors). BMS708163 is developed by Pfizer for AD treatment (Avagacestat) and the Company claimed a theoretical better outcome over Semagacestat (LY450139) [125], whose trials in AD were stopped for side effects (skin tumors) and worsening of cognitive performances (likely due to its not specific activity on other γ-secretase substrates like Notch), because it should be more selective versus APP than on Notch.

However, also Avagacestat recently failed in a clinical trial in prodromal AD patients, showing severe adverse effects (principally, non-melanoma skin cancer) and worsening of cognitive capabilities [126]. Another γ-secretase inhibitor, RO4929097 is currently studied in clinical trial in cancer and there are no information about AD [30,125,127,128]. Besides APP and Notch, no data are available relatively to their activity on the processing of LRP8 or other γ-secretase substrates.

The efficacy of the inhibitory activity of these compounds was attested by SDS-PAGE and WB experiments on N2A stably expressing hHA-LRP8. Using an antibody anti-C-terminus of APP (Zymed) to ascertain the effect of γ-secretase inhibitors, we observed, in treated cells, an increment of APP fragments migrating at 12 kDa (C99 fragments), which are the substrates of γ-secretase, after β-secretase cleavage. As expected, the accumulation of C99 is a marker of γ-secretase inhibition (**Figure 12 A**).

On the other side, γ-secretase inhibitors cause an increment of the fragment of LRP8 migrating between 20 and 25 kDa or LRP8 C-terminal fragment, that represents the γ-secretase substrate, as reported in the literature [104,112] (**Figure12 B**), indicating an inhibitory effect of these drugs also in the “canonical” processing of LRP8. However, we also observe that there is an increment of shorter fragments (LICDs) upon treatment with γ-secretase inhibitors. This event is surprising because we would expect a reduction of LICDs, as being products of γ-secretase. Not all inhibitors induce the same effect on LRP8 and on LICDs and this effect could be due to a different IC50 that each drug may have on LRP8 (**Figure 12 B**).

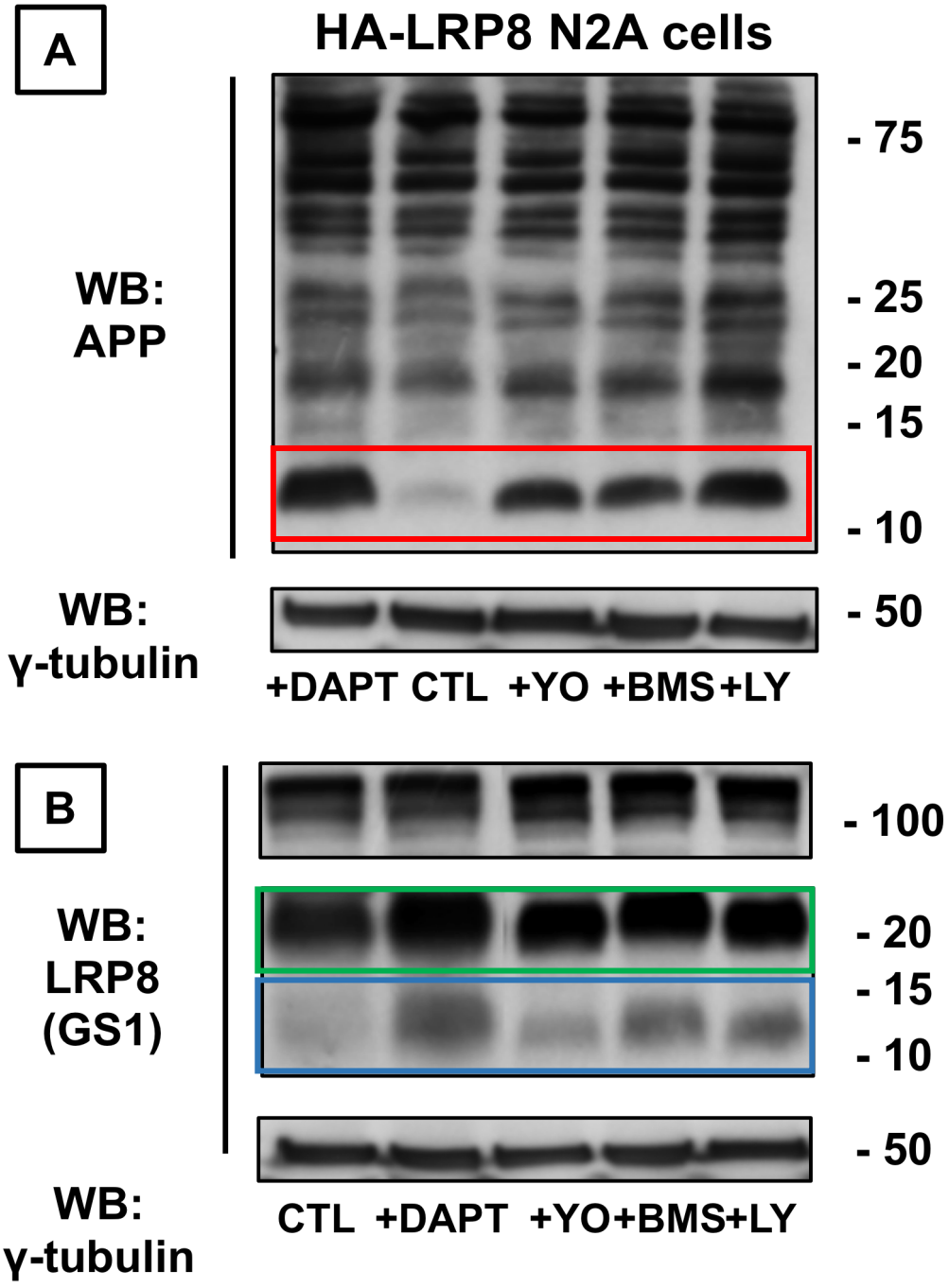

Figure 12 – WB of cell lysates from N2A cells, stably expressing HA-LRP8, treated with different γ-secretase inhibitors. (A) Upper WB is probed with an anti-C-terminus of APP (Zymed) for APP and its C-terminal fragments (C99) identification: red box evidences the accumulation of C99 in N2A HA-LRP8 treated with γ-secretase inhibitors (10 μM, 16 hrs). (B) Lower WB is probed with GS1 to study LRP8 FL and LICDs: green box evidences the increase of LRP8-γ-secretase substrate,

while blue box indicates the accumulation of LICDs despite the inhibition of γ-secretase activity. CTL are control cells, vehicle treated: PBS+DMSO 0,1%. YO=YO01027, BMS=BMS708163, LY=LY450139.

Densitometric analysis (ImageLab) shows that YO01027 and LY450139 (Semagacestat) are less efficient in increasing LICDs than BMS708163 or DAPT, which all up-regulate LICDs (**Figure 13 A**) strongly and significantly (red asterisks) in comparison to vehicle-treated cells (PBS+0.1% DMSO). DAPT treatment is statistically significant vs. all the groups treated with the other γ-secretase inhibitors (black asterisks), while BMS708163 treatment is statistically significant (green asterisks) vs. YO01027 and LY450139 treatments ($p<0.05$). Furthermore, as observed with APP, also the fragments migrating between 20 and 25 kDa, that are the real substrate of γ-secretase, are significantly accumulated (**Figure 13 B**) in respect to the vehicle-treated cells (red asterisks), indicating inhibitory effects of these drugs also on LRP8 processing.

All these data reveal interesting and surprisingly results: LICDs are accumulated in cells treated with γ-secretase inhibitors, with a parallel accumulation of C99 and LRP8 fragments of 20-25 kDa. Considering that LICDs are fragments migrating between 8-12 kDa and considering the sequence of LRP8 (we do express isoform 1, the longest, Uniprot: Q14114-1), there is no possibility that these fragments are substrates of γ-secretase because, as reported, the MW of γ-secretase product is ~15 kDa.

Interestingly, LICDs are accumulated after treatment with γ-secretase inhibitors also in N2A wt that has endogenous levels of mouse isoforms of LRP8, indicating that this differential processing could be conserved also in other species and that the effect exerted by γ-secretase inhibitors is present also on wild type protein (**Figure 14**).

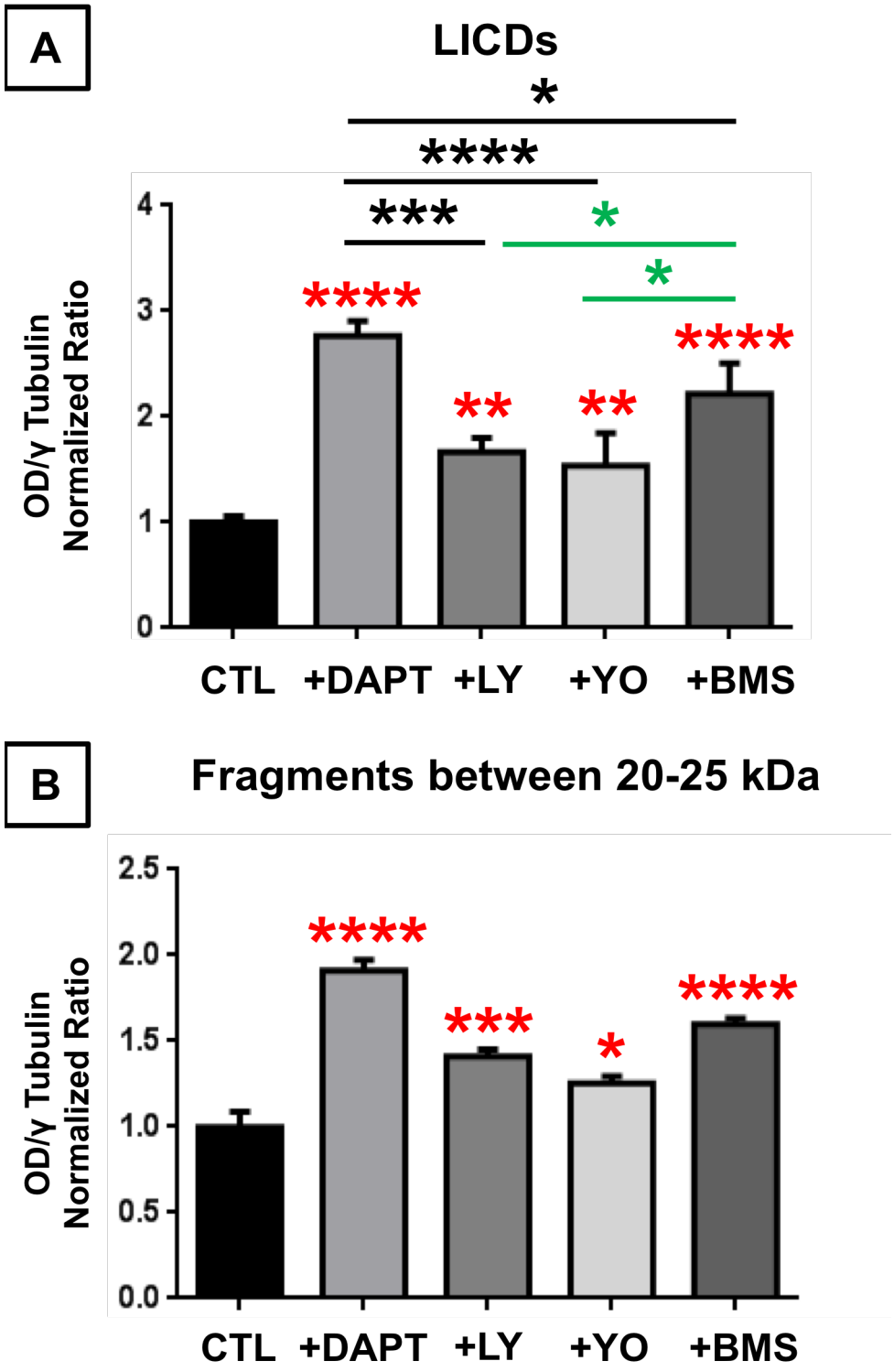

Figure 13 – Densitometric analysis of N2A stably transfected with HA-LRP8 and treated with γ-secretase inhibitors reveal an accumulation of LICDs (A) and fragments between 20-25 kDa (B) significantly higher vs. control group, in particular with DAPT and BMS708163. For both class of fragments DAPT treatment is significantly higher respect all the other groups. CTL are control cells, vehicle treated: PBS+DMSO 0,1%. YO=YO01027, BMS=BMS708163, LY=LY450139.

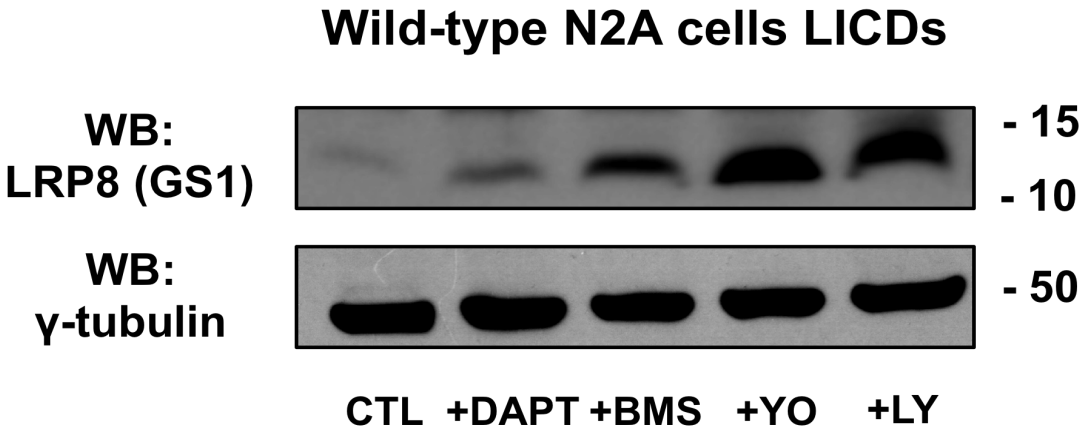

Figure 14 – N2A wt cells treated with different γ-secretase inhibitors reveal a significant accumulation of LICDs produced by the endogenous LRP8.

Consequences of LICDs increment upon γ-secretase inhibition

The theoretical C-terminal fragment produced upon γ-cleavage is: I A L L C M S G Y L I W R N W K R K N T K S M N F D N P V Y R K T T E E E D E D E L H I G R T A Q I G H V Y P A A I S S F D R P L W A E P C L G E T R E P E D P A P A L K E L F V L P G E P R S Q L H Q L P K N P L S E L P V V K S K R V A L S L E D D G L P, which should have a MW of 15kDa, as reported also in the literature.

The minimum sequence detectable by GS1, starting from its epitope (underlined) should be the following: <u>D E D E L H I G R T A Q I G</u> H V Y P A A I S S F D R P L W A E P C L G E T R E P E D P A P A L K E L F V L P G E P R S Q L H Q L P K N P L S E L P V V K S K R V A L S L E D D G L P, with a MW of about 10 kDa.

In any case, an increment of both sequences should be due to an enhancement of γ-secretase activity, rather than a block, as expected using γ-secretase inhibitors.

These results elicit different questions:

1- **Are LICDs real products of γ-secretase? Or rather other enzyme(s) may generate them, mostly when γ-secretase is blocked?**

2- Are maybe the inhibitors tested not active on a specific pool of γ-secretase that processes LRP8?

To answer to the first question, we made specific experiments on MEF cells derived from mice wild type or mice *PSEN-1/2* double KO. We transfected these cells with LRP8 ddk-myc-tagged and we analyzed its processing by SDS-PAGE and WB. The aim was to verify whether LICDs can be formed even in absence of PSEN-1/2 and, consequently, of γ-secretase activity.

In these experiments, we can observe that LRP8-ddk-myc is equally expressed in wild type cells as well as in PSEN-1/2 KO cells (as evidenced by the signal at ~100 kDa), after transfection. Interestingly, C-terminal fragments of LRP8 are produced in both transfected cell lines (~20 kDa), and LICDs (red box) are produced even in absence of active γ-secretase (MEF *PSEN-1/2* double KO) (**Figure 15**), further confirming that LICDs are not γ-secretase products. There is an a-specific signal present in both transfected and non-transfected cells as a single band migrating at about 25 kDa.

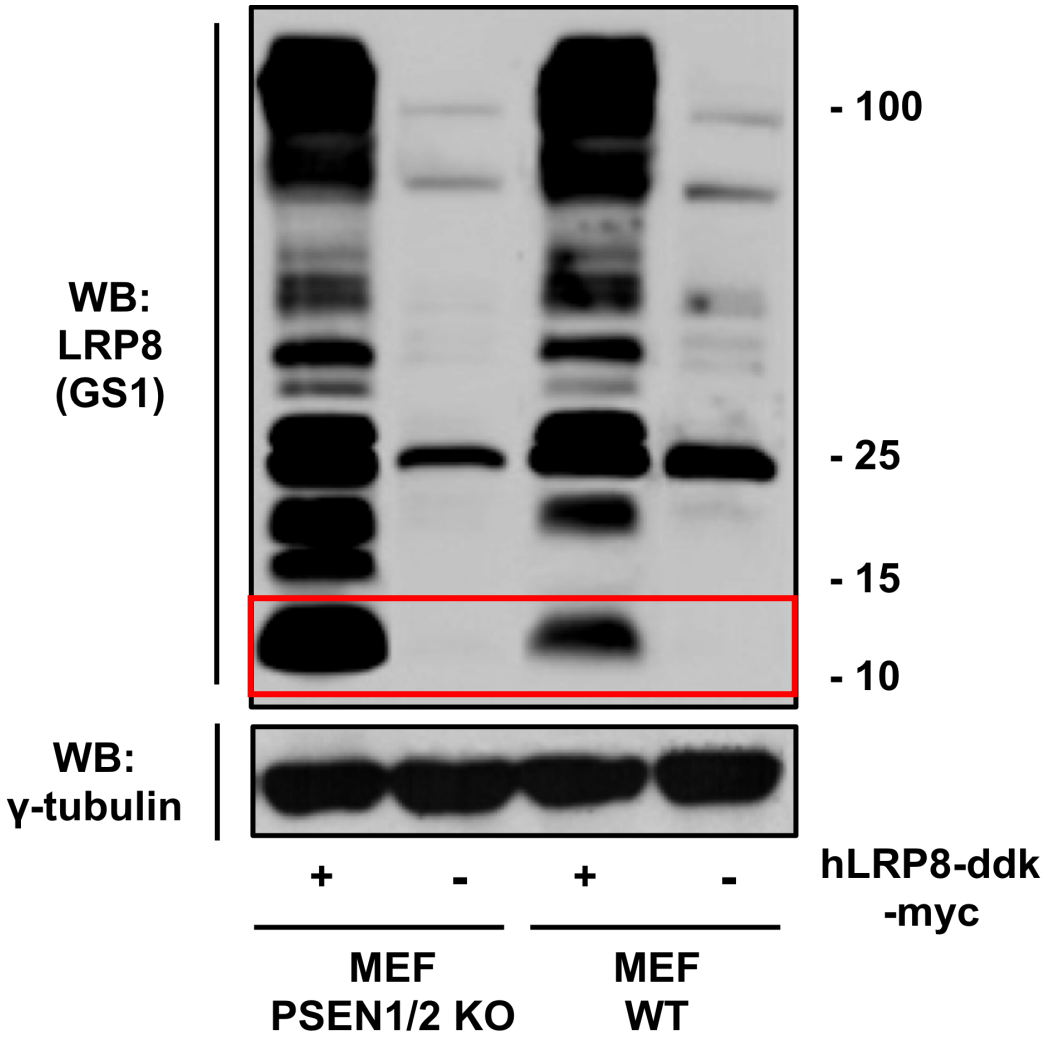

Figure 15 – MEF wt and PSEN-1/2 KO cells were mock or human LRP8-ddk-myc transfected. Cell lysates were analyzed by SDS-PAGE and WB, with GS1 antibody, for LRP8 recognition. LICDs are present only in transfected cells, even in *PSENs* KO cells (red box).

C-terminal LRP8 without the sequence of γ-secretase cleavage is processed like LRP8 FL

Starting from the observation that LICDs are produced even when γ-secretase is not functional (MEF PSEN-1/2 double KO), we used a construct expressing LRP8 C-terminal sequence that does not have the cleavage sequence of γ-secretase, but that partially conserves the transmembrane sequence so that this fragment could be

located in the plasma membrane, where it could be processed as the FL. In **Figure 16 A** are reported the sequence of LRP8 isoform 1 and C-terminal LRP8 construct (C-Term LRP8).

In WB experiments (**Figure 16 B**), we analyzed the processing of C-Term LRP8: it should produce a fragment of about 15 kDa, similar to the C-terminal fragment produced by γ-secretase, as previously reported [104]; while we detect a band of about 18 kDa (green box), that is present also in N2A transfected with the LRP8 FL (green arrow). Noteworthy, C-term-LRP8 is ddk-myc tagged, therefore its apparent MW is increased of about 3 kDa, in comparison to the endogenous wild type form. C-Term LRP8, when is transfected in N2A wt, showed a comparable processing to that of N2A transfected with the LRP8 FL, producing LICDs (red box), that are increased when treated with DAPT (control cells were treated with PBS+0.1% DMSO), analogously to previous showed data with LRP8 FL. It is possible to speculate that C-Term LRP8 sequence is very similar to that of the 18kDa fragment produced by the FL processing.

Furthermore, ICC experiments were performed on N2A cells transfected with C-Term LRP8 and EGFP to study the intracellular localization of this fragment; as hypothesizes, ICC revealed that C-Term LRP8 (red signal, white arrows) is localized also to the plasma membrane of EGPF-positive transfected cells, suggesting that this fragment can be processed as the endogenous pool (**Figure 16 C**).

In conclusion, these results clearly suggest that LICDs are produced even in absence of γ-secretase and that may be produced even from γ-secretase-derived fragments (C-Term LRP8). As a consequence, we could suppose that LRP8 has a dual processing: one is normally mediated by γ-secretase while, when γ-secretase is hampered (see inhibitors) or less efficient (mutations and loss-of-function as in AD brain?), LRP8 membrane-bound fragments are processed, likely by other enzymes, leading to an increment of LICDs.

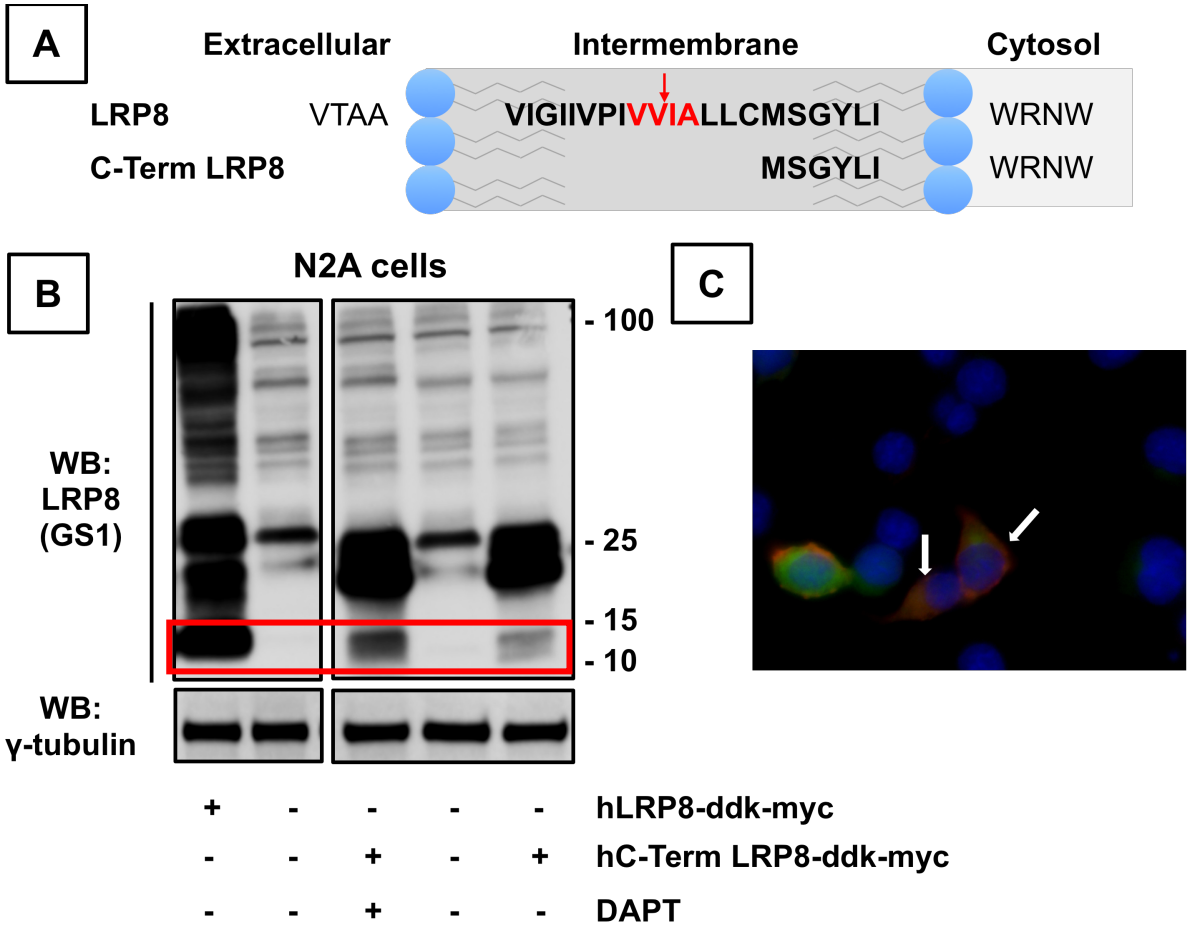

Figure 16 – (A) Schematic detail of the intermembrane sequence of hLRP8-ddk-myc and C-Term LRP8-ddk-myc. (B) Representative WB of proteolytic processing of N2A wt, transfected with human LRP8-ddk-myc and C-Term LRP8-ddk-myc. C-Term LRP8-ddk-myc (green box) shows a similar pattern in the proteolytic processing of LICDs compared to N2A transfected with the full-length of LRP8 (green arrow and red box). DAPT treatment seems to accumulate more LICDs in N2A transfected with C-Term LRP8. **(C) ICC experiments performed on N2A transfected with C-Term LRP8 (red) reveal a plasmamembrane localization in EGFP-positive cells (green) with nuclear DAPI stain (blue).**

RESULTS

PART III

Inhibitors of proteasome and of histone deacetylase Tip60/Kat5 decrease LICDs in vitro

As described previously, LRP8, exactly as APP, is a receptor involved in cell-signalling events. In particular an important interactor of LRP8 (and APP) is Tip60/Kat5, along with FE65. Tip60/Kat5 is an histone acetyltransferase linked to APP and likely LRP8 signalling, and is involved in learning and memory processes, as well as in DNA repair [102,129–131]. The interaction between APP/FE65/Tip60 is rather complex and its transcriptional activity may be both γ-secretase dependent or independent [130]. It is in any case peculiar and interesting the possibility that Tip60/Kat5 shuttling from membrane to the nucleus may be conditioned by APP and/or LRP8 processing [132].

Therefore, we explored the possibility that an inhibitor of Tip60/Kat5 (NU-9056) would affect LRP8 processing and LICDs formation. In parallel, we analyzed the effect of a common and relatively a-specific inhibitor of proteasome and other proteases, such as ALLN, a cell permeable peptide aldehyde inhibitor of calpain I and to a lesser extent calpain II. Also, it inhibits other neutral cysteine proteases, cathepsin B and L and the proteasome.

Both treatments (20 μM per 16 h) induce a reduction of LICDs (red box) and a parallel increment of the 20-25 kDa fragment (green box) (**Figure 17**). Thus suggesting that LICDs are produced by non-γ secretase proteases (neither NU-9056 nor ALLN are known to inhibit γ-secretase) and under the control of Tip60/Kat5, suggesting thus a potential transcriptional role for LICDs [104].

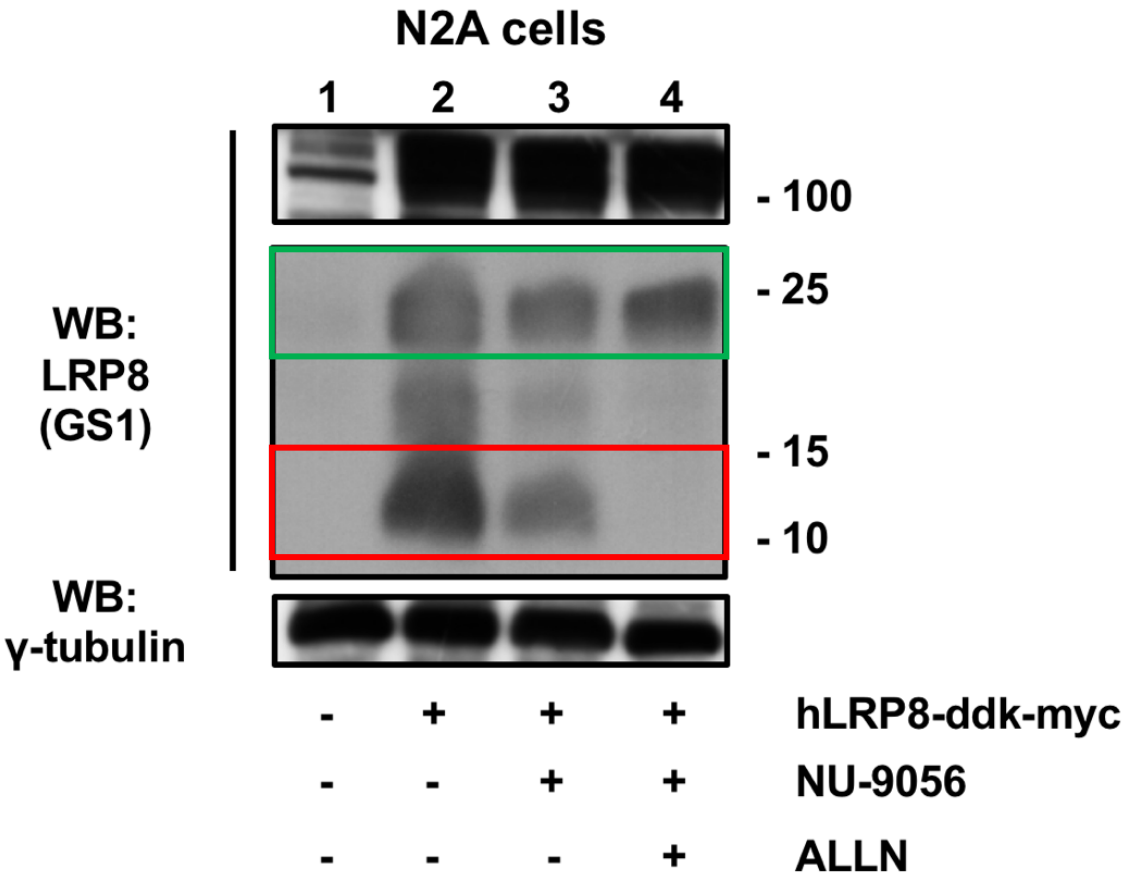

Figure 17 – Representative WB with GS1 antibody on cell lysates from N2A wt vehicle treated (PBS+DMSO 0,1%) (1) and LRP8-ddk-myc transfected cells (2-4) differentially treated with a Tip60/Kat5 inhibitor (NU-9056) and a inhibitor of proteasome (ALLN). These experiments reveal that the use of these drugs reduce or nullify the accumulation of LICDs (red box), while cause an increment of 20-25 kDa fragment (green box).

In silico studies to identify possible proteases involved in the alternative LRP8 processing

Previous reports suggested the involvement of specific proteases in the course of AD, either as cause for neurodegenerative or inflammatory processes, or as consequence of Aβ-induced degeneration [133–135]. The complex proteolytic machinery required for APP homeostasis relies on metallo-proteases (ADAM family),

aspartyl endopeptidase (memapsin 2 or BACE1), and on iCliPS made by γ-secretase. However, other proteases can potentially cleave APP [136,137], with a yet unclear role in AD.

Considering the potential involvement of the processing of LRP8 in AD genesis, and the likely role of other non-γ-secretase proteases on its processing, we made an *in silico* analysis, using the "MEROPS" database (https://www.ebi.ac.uk/merops/), looking for proteases potentially able to cleave LRP8 intracellular sequence, among those proteases known to interact or cleave APP. We identified 8 proteases that could be involved in the "alternative" processing of LRP8 (**Figure 18**), among those reported to have an activity on APP processing, and/or with a putative involvement in AD pathogenesis.

Here we report the list of proteases studied:

- **ADAM's cleavage (mainly the most studied ADAM10 and ADAM17)** in AD is considered a protective event since it is nonamyloidogenic in the APP processing. However, considering the "cell-cycle" hypothesis, an increment of α-secretase may be not so positive.

- **ADAMTS-1** is a disintegrin and metalloprotease with thrombospondin 1 (TSP1)-like motifs with ubiquitous expression. Proteoglycans are its natural substrates and KO mice models suggest that may be involved in cell growth, fertility, organ structure and function. The gene is encoded on chromosome 21, as for APP, and its levels are up-regulated in Down's syndrome and in AD brain samples [138].

- **Matrix metalloprotease 9 (MMP9)** positively regulates synaptogenesis and plasticity mechanisms; however, an increased activity of MMP9 is detected in AD brains [139]. Additionally, MMP9 was found in pyramidal neurons of AD brains and near amyloid plaques; it was shown that MMP9 is able to cleave Aβ_{40} [135]. Whether this is a protective condition (improved degradation of Aβ) or not (ECM degradation and inflammation) has to be clarified.

- **Meprins (Meprin α and β)** are Zn^{2+}-dependent proteases of the astacin family, known for being over-expressed in different tumors and, only recently, are described as proteases cleaving the N-terminal portion of APP (essentially Meprin β), principally generating aggregation-prone N-terminally truncated Aβ peptides; in particular, N-terminally truncated $Aβ_{2-40}$ variant shows increased aggregation propensity compared to $Aβ_{40}$ and acts even as a seed for $Aβ_{40}$ aggregation [133,137,140–143]. *MEP1A* and *MEP1B* genes encode respectively for Meprin α and β.

- **Cathepsins (in particular Cathepsin D and L)** are intracellular acidic proteases which cleave APP and can be over-expressed and secreted in pathological conditions related to neurodegeneration: Cathepsin D, which accumulates within AD neurons, also cleaves at the N-terminal side of the first aspartate residue of amyloid β [136,144,145]. Furthermore, ALLN is active to inhibit this family of proteases. *CTSD* and *CTSL* genes encode respectively for Cathepsin D and L.

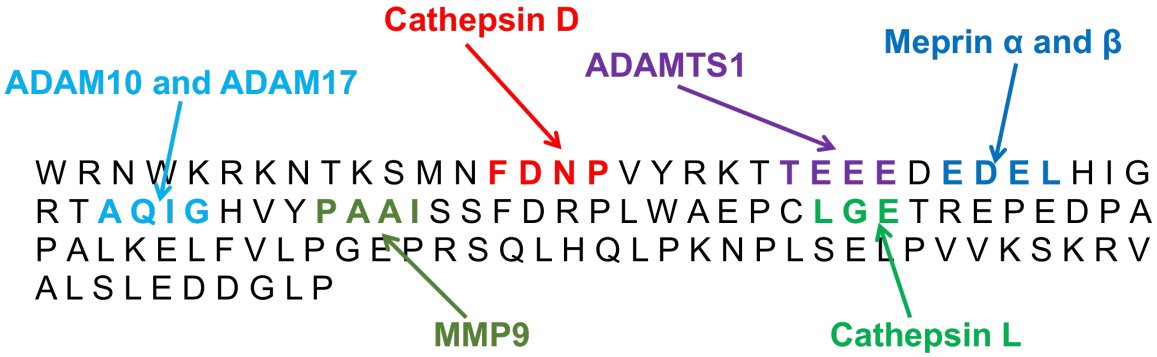

Figure 18 – *In silico* analysis of putative processing sites by "alternative" proteases in the intracellular domain of LRP8, using MEROPS database. Hypothetical fragments produced by Cathepsin D, ADAMTS1 and Meprins have a molecular weight between 10 and 11 kDa.

ADAM10, ADAM17, ADAMTS1, CTSD, CTSL, MEP1A, MEP1B and MMP9 mRNAs expression in human frontal and temporal cortices

In order to assess whether the gene expression of these proteases (the two α-secretases *ADAM10* and *ADAM17, ADAMTS1, CTSD, CTSL, MEP1A, MEP1B and MMP9*) in brain samples from SAD and non-demented control patients, we performed a comparative analysis of the mRNAs expression levels in the frontal and temporal cortices specimens of each patients, using qPCR experiments. For each gene analyzed, RQ values (normalized by the two housekeeping genes *EIF4A2* and *GAPDH,* software: RQ Manager 1.2), were normalized to respective control group mean value.

Among the α-secretases, we found that *ADAM10* mRNA expression is significantly ($p<0.05$) 1.72-fold higher (controls=1,00±0,17 vs. SAD=1,72±0,18) in SAD (n=10) compared to the control (n=14) subjects (**Figure 19 A**). Values in the two groups are independent from age. On the other side, mean values for *ADAM17* (controls=1,00±0,22 vs. SAD=0,99±0,16) are similar (p=0,97) between the groups (SAD n=11; controls n=14) (**Figure 19 B**).

We found a statistically significant difference between groups only for the mRNAs expression of mRNAs expression of *ADAMTS1* ($p<0,05$), *CTSD* ($p<0,0001$) and *MEP1B* ($p<0,05$) (**Figure 19 C, D, G**). In detail, *ADAMTS1* was about 2,08-fold higher (controls=1,00±0,24 vs. SAD=2,08±0,39) in SAD samples (n=10) compared to the control group (n=14) (**Figure 19 C**); *CTSD* was 2,96-fold higher (controls=1,00±0,17 vs. SAD=2,96±0,35 in SAD samples (n=10) compared to the control group (n=14) (**Figure 19 D**); while *MEP1B* was 1,67-fold higher (controls=1,00±0,16 vs. SAD=1,67±0,21) in SAD specimens (SAD n=10; controls n= 15) (**Figure 19 G**). The mRNA expression levels of *CTSL*, *MEP1A* and *MMP9* did not differ (p=0,60, p=0,71 and p=0,58, respectively) between SAD and control samples (**Figure 19 E, F, H**). In detail, *CTSL* - controls=1,00±0,15 vs. SAD=1,13±0,20 - (SAD n=10; controls n=14); *MEP1A* - controls=1,00±0,32 vs. SAD=1,16±0,30 - (SAD n=10; controls n=13); and *MMP9* - controls=1,00±0,40 vs. SAD=1,34±0,45 - (SAD n=10; controls n=13) (**Figure 19 E, F, H**).

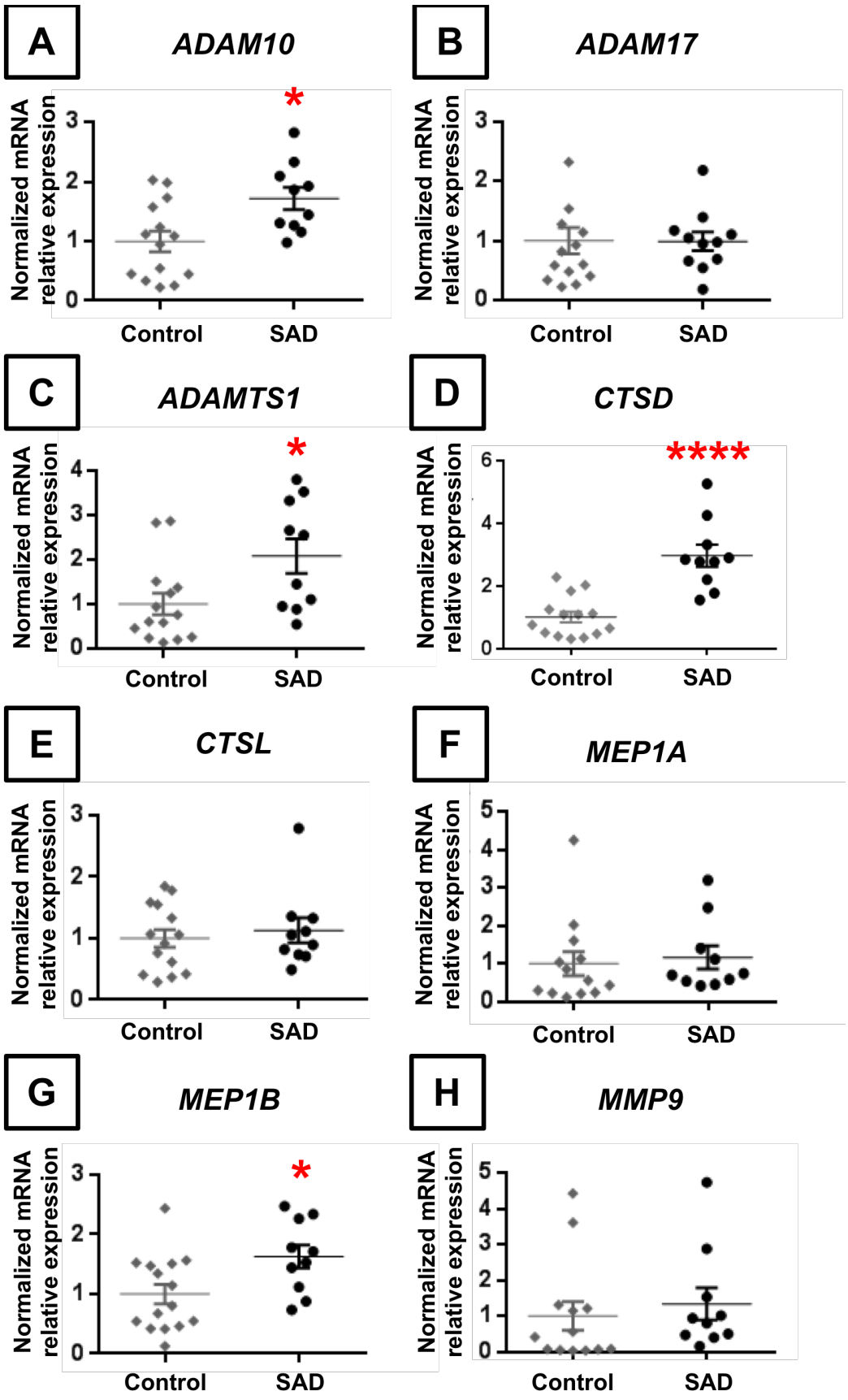
A
ADAM10
Normalized mRNA relative expression
*
Control
SAD
B
ADAM17
Normalized mRNA relative expression
Control
SAD
C
ADAMTS1
Normalized mRNA relative expression
*
Control
SAD
D
CTSD
Normalized mRNA relative expression
****
Control
SAD
E
CTSL
Normalized mRNA relative expression
Control
SAD
F
MEP1A
Normalized mRNA relative expression
Control
SAD
G
MEP1B
Normalized mRNA relative expression
*
Control
SAD
H
MMP9
Normalized mRNA relative expression
Control
SAD

Figure 19 – Proteases mRNA expression in cerebral cortex of control non-demented and SAD patients: *ADAM10* (A), *ADAM17* (B), *ADAMTS1* (C), *CTSD* (D), *CTSL* (E), *MEP1A* (F), *MEP1B* (G) and *MMP9* (H). Only *ADAM10, ADAMTS1, CTSD* and *MEP1B* are significantly higher expressed in SAD patients than in control non-demented subjects. Each symbol represents the mean value of a single patient.

ADAMTS1, Cathepsin D and Meprin β protein expression in human frontal and temporal cortices

In the literature there are rare and anecdotal information about the expression levels in human brain of the above-mentioned proteases, relatively to both mRNA and protein. Evaluating our data and the sequence of C-term LRP8 (see **Figure 18**), it appears that among the proteases whose mRNA is increased in AD patients, only ADAMTS1, Cathepsin D and Meprins can produce LICDs fragments detectable by GS1 antibody, since their cleavage sites are in the range of its epitope: D E D E L H I G R T A Q I G. ADAM10/17, MMP9 and Cathepsin L cleavages would instead produce fragments not normally detectable by GS1.

For these reasons, we focused our attention on ADAMTS1, Cathepsin D and Meprin β protein expression, evaluating their protein levels by SDS-PAGE and WB analysis in the same brain samples used in qPCR experiments (**Figure 20 A**).

Cathepsin D undergoes proteolytic cleavage and activation mainly by ADAM30, producing two chains (light and heavy) that are reassembled in the active isoform by disulfide bonds: the anti-Cathepsin D antibody used in this study is able to detect both the pro-Cathepsin D isoform (migrating at 52 kDa) and the heavy chain of Cathepsin D (or active isoform, migrating at 26 kDa, upon cleavage of disulfide bridges) in denaturant conditions [146,147].

Protein expression levels were normalized measuring the level of the highly stable γ-tubulin protein in each sample and its mean value in the control group. Data obtained (**Figure 20 B**) show ADAMTS1 protein expression level in SAD patients (n=12) was 4,13-fold higher ($p<0,0001$) in comparison to controls (n=15): 4,13±0,27 vs.

1,00±0,15. pro-Cathepsin D and Cathepsin D (heavy chain), are expressed 3,08- (p<0,01) and 2,80-fold times (p=0,0001) in SAD patients (n=13) vs. non-demented subjects (n=12): 3,08±0,64 vs. 1,00±0,26 and 2,80±0,36 vs. 1,00±0,16, respectively, suggesting that the higher expression of Cathepsin D is not limited to its precursor: this observation suggests an increased availability of active isoform in AD brain. Meprin β protein expression level was 1.9-fold higher (p<0,01) in SAD subjects (n=13) in comparison to non-demented subjects (n=15): 1,90±0,24 vs. 1,00±0,14.

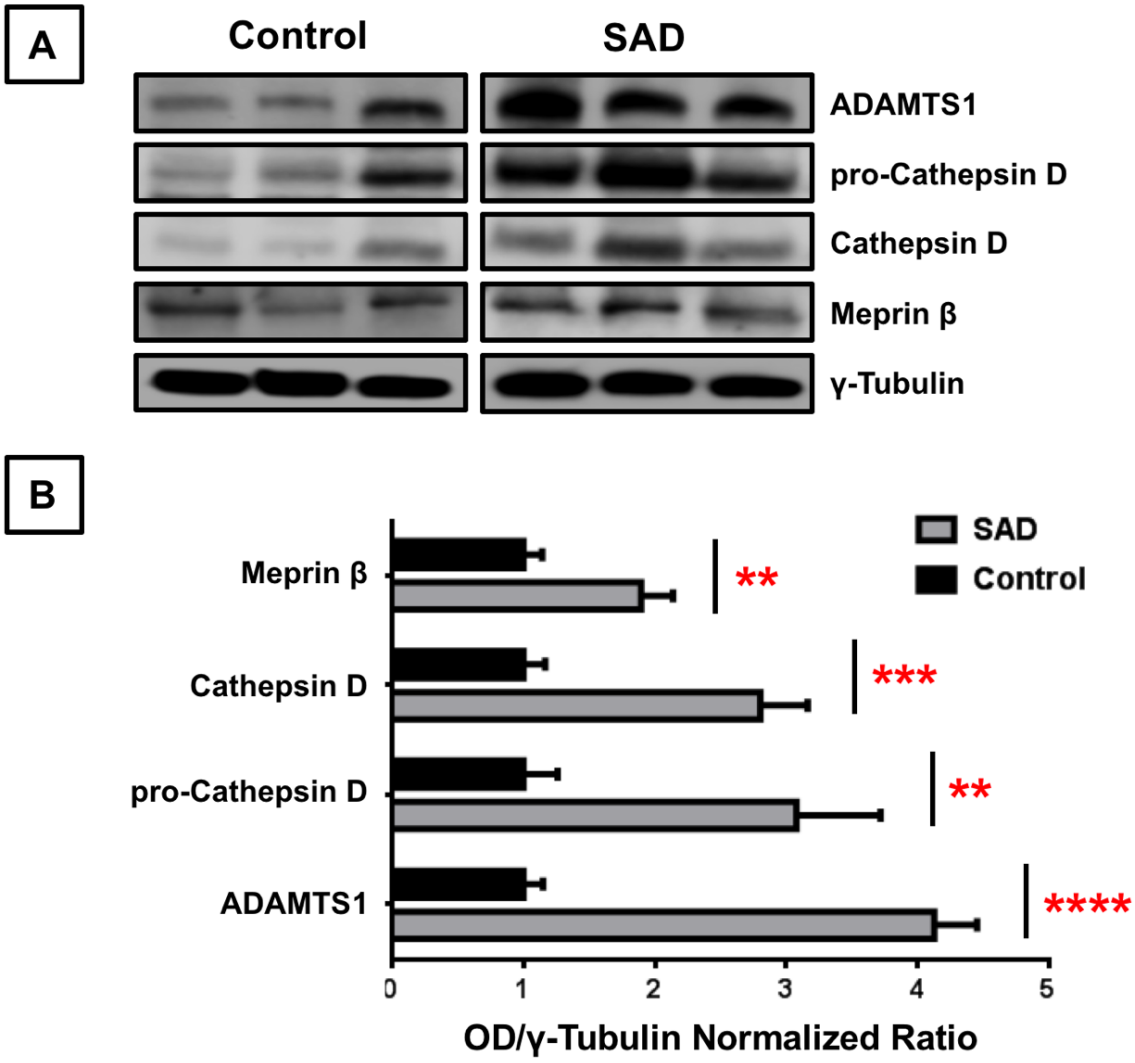

Figure 20 – (A) Representative WB of protein proteases level of ADAMTS1, pro-Cathepsin D, Cathepsin D (active isoform, heavy chain) and Meprin β. (B) Densitometric analysis reveals significant higher levels of proteases analyzed. ADAMTS1 is 4,13-fold higher (p<0,0001), pro-Cathepsin D and Cathepsin D isoforms

3,08- ($p<0,01$) and 2,80- ($p=0,0001$) fold and Meprin β 1,90-fold higher ($p<0,01$) in SAD group in comparison to non-demented group.

DISCUSSION

Clinical failure of trials based on the “amyloid hypothesis” (either using antibodies vs. Aβ or using γ-secretase inhibitors/modulators) [148] along with discrepancies in the theory caused by recent studies on γ-secretase “loss–of-function” [44,45], pushed into a revision of the theory. In this scenario, it is still unclear whether the potential “loss-of-function” of γ-secretase, that may occur in course of AD, may be relevant also for other substrates, besides APP.

Among different γ-secretase substrates, in this thesis we focus on LRP8 (or ApoER2), the only one that possesses peculiar features potentially relevant for AD genesis: it is an APP’s interactor modulating Aβ formation; it is expressed at neuronal level; it is a receptor for ApoE (which is the most important risk factor for developing AD); it is involved in signalling activities such as neuronal migration or cell proliferation and memory processes, sharing with APP common adaptors and ligands [86,91,104,112–115]; it has a complex processing, as APP, sharing with APP exactly the same consensus site for γ-cleavage in the transmembrane sequence (V V - I A).

Little is known about the processing of LRP8 in human, most of information derive from *in vitro* studies and experiments on mice [104,110,149,150]. Our experiments were initially performed in brain samples from control non-demented subjects, patients with sporadic form of AD, and patients with familial AD (bearing mutations on *PSEN-1*), to verify the expression pattern and processing of LRP8 in different conditions. In particular, studying FAD subjects, we had the opportunity to explore LRP8 levels and its processing in a very severe pathological condition and linked to a system in which γ-secretase is dysfunctional due to mutations in *PSEN-1*.

In the literature, LRP8 processing is described in a few papers that indicate a first cleavage by a yet unclear sheddase (likely a furin-like cleavage) to form 20-24 kDa fragments further processed by γ-secretase producing 15-18 kDa C-terminal fragments, similar to AICDs formed upon APP cleavage [104,112]. In this study we observe significant differences between control cases and demented patients: *in primis* a significant reduction of the full-length LRP8 isoforms migrating at 100-105 kDa, with a concomitant increase of small fragments of about 8-12 kDa (collectively called LICDs and that to-date have never been reported in the literature).

In a previous work, full-length LRP8 expression was reported as unchanged in frontal cortex of AD patients, however in that study there is a huge difference on average ages between groups, while our subjects are completely age-matched [151].

The first observation regards the nature of LICDs, the MW in SDS-PAGE of which is much smaller than that foreseen for the products of the action of γ-secretase on LRP8 (15 kDa) or for those previously described in the literature, where are often shown as migrating between 15-18 kDa. These aspects are investigated in the second part of this thesis, in which we describe LICDs of 12 kDa produced in cells treated with inhibitors of γ-secretase, in MEF cells double KO for PSENs and even in cells expressing an engineered construct that exactly expresses the product of γ-secretase cleavage with a theoretic MW of 18 kDa (15 kDa plus 3 kDa tag) (see **Figure 16**). Altogether, these data suggest that, beside γ-secretase, other cleavages may occur on LRP8, and that shorter fragments are produced in special conditions:

a) in pathological conditions such as in SAD and FAD brains (**Figures 6-8**), and
b) when γ-secretase is blocked or absent (**Figures 12-16**).

The analysis of human brain shows that the overall level of LRP8 (full length and C-terminal fragments, together) is similar between controls and demented subjects; therefore, the relative reduction of full-length protein and the parallel increment in C-terminal fragments - in SAD and FAD subjects only -, can be ascribed to an enhanced processing rather than a reduced synthesis. This is also confirmed by our in vitro experiments, in which LICDs are induced, while full-length protein expression is stable. Complexity arises when we consider the question whether in demented patients, from the pathological point of view, it may be more relevant the decrement of full-length protein than the increase in LICDs.

LRP8, as a receptor, has a plethora of function in human brain, important for neuronal migration, cholesterol homeostasis and memory processes [89,104,106,113]. A reduction of its levels may be a relevant issue during ageing. As far as the increment of LICDs concerns, the situation is even more complicated, since, as for AICD, the literature is somehow non-homogeneous about their uncertain

transcriptional role. A third hypothesis is that both features may be relevant in AD, as they may be implicated in mechanisms that maintain or induce degeneration in neurons. The abnormal processing of LRP8 is not present in those few non-demented subjects bearing plaques and staged III in Braak & Braak classification (cases 3216 and 963), while it is detectable also in the cerebellum of SAD patients with late-stage of AD (V-VI stage in Braak & Braak classification). These feature suggest a possible correlation between severity of the disease and abnormal processing of LRP8, as previously shown for specific Aβ fragments bearing N-terminal modifications [48].

Of course, it is likely that the abnormal processing of LRP8 observed in SAD and FAD patients in comparison to non-demented subjects is a consequence of the disease, rather than being a cause. However, the relative misplacement of LRP8 - in SAD and FAD brains in comparison to controls (see **Figure 9**) - from neurons to a rather diffuse parenchymal staining, suggest also a pathological correlation: LRP8 staining is present in healthy neurons, while NFT bearing neurons are void of LRP8.

It is conceivable to speculate that the diffuse parenchymal staining shown by GS1 antibody, could be due to the neuronal degeneration that occurs in AD patients. This feature might be again only a consequence of neuronal failure. Besides, (considering also the experiments on human cerebrospinal fluid and plasma) it appears that LRP8 and its LICDs could be also observed as potential markers of the disease. At present it is very difficult to give a reasonable interpretation about the finding that LICDs are increasingly present in plasma and cerebrospinal fluid of demented patients (even in their early stage - see MCI patients in **Figure 11**), while they are undetectable in samples from age-matched control subjects. Currently, the small number of samples does not allow any type of speculation. The only observation is that the parenchymal distribution of LRP8/LICDs in SAD and FAD patients, might be reflected in cerebrospinal fluid samples. Unfortunately, the antibody GS1 cannot distinguish in IHC experiments between LRP8 holoprotein and LICDs; therefore, we can only speculate that the increment of extracellular signal shown in SAD and FAD patients (**Figure 9**), if attributable mainly to LICDs, may also cause a higher cerebrospinal fluid/plasma content of LICDs, as shown in **Figures 10-11**.

Another important issue concerns the concept of “loss-of-function” regarding *PSENs*. In this thesis we show that FAD patients bearing mutations on *PSEN-1* gene, characterized by early onset and very severe phenotype, have a significant increment of LICDs. The same feature is detectable in cultured cells when γ-secretase is blocked either using specific drugs (**Figure 12**) or in cells in which PSENs are KO (**Figure 15**). Therefore, it is tempting to speculate that a failure of γ-secretase, or a loss-of-function - here induced pharmacologically, there by a point mutation - is responsible for the observed phenotype. Interestingly, similar effects are obtained on endogenous LRP8. The acute single-dose use of γ-secretase inhibitors (YO01027, LY450139, BMS708163 and DAPT) cause an accumulation of C99 and LRP8 fragments of 20-25 kDa in N2A cells stably transfected with HA-LRP8. This data are coherent with the literature: BMS-708163 (Avagacestat) acute single treatment (4 h) in rats causes an accumulation of C99 (and this effect could be extended also to LRP8 and other substrates), while a prolonged treatment causes a reduction of C99 and C-terminal fragments of LRP8, due to an enhanced expression of *PSEN-1* mRNA [152]. Also an inactivation of γ-secretase cause an increase of membrane-bound fragments of APP, Deleted in Colorectal Cancer and LRP1 [153].

However, there is here a conceptual Gordian knot: if γ-secretase activity is hampered, why LICDs are produced and even increasingly? Interestingly, our data show that LICDs migrate at a low MW, lower than that foreseen upon γ-secretase cleavage on LRP8 membrane-bound fragments. Moreover, their formation is independent on γ-secretase (as shown in *PSENs* KO cells) and can be formed from an artificial precursor whose sequence begins after the γ-site (C-term LRP8, **Figure 16**).

Altogether, these data strongly suggest that LICDs may be produced by a non-γ secretase activity. Even that they can be over-produced when γ-secretase activity is reduced or hampered.

In this scenario, we should, therefore, hypothesize that a γ-secretase’s “loss-of-function”, such as in familial patients bearing *PSEN-1/2* mutations or in cells treated

with γ-secretase inhibitors, makes LRP8 available to other proteases which cleave LRP8 even more efficiently than PSENs itself. Keeping this in mind, it is not a surprise the failure of therapeutic approaches using γ-secretase inhibitors.

Recently, in the literature, it was reported that a PSEN-1 R278I mutation showed impaired γ-secretase activity concerning LRP8 processing: WB experiments revealed an accumulation of both LRP8 sheddase (~22 kDa) and γ-secretase (~18-19 kDa) products, while lower fragments are not reported, maybe because commercial antibodies are not able to detect smaller fragments. DAPT exposition caused a significant accumulation of LRP8 fragments, even in the absence of PSEN-1 mutation, compared to the vehicle-treated cells, as reported in our experiments too (**Figure 12**) [112].

The last issue explored in this thesis regards the role of non-γ-secretase proteases in LRP8 processing. In our experiments an inhibitor of Tip60 (NU-9056), the acetylase involved in AICD trafficking and signalling [130], partially reduced the formation of LICDs *in vitro*. Adding a relatively a-specific inhibitor of proteasome and other proteases, such as ALLN, we blocked the formation of LICDs increasing its precursors (**Figure 17**). Considering that neither ALLN nor NU-9056 are able to block γ-secretase, these data confirm that LICDs are produced by a non-γ cleavage, that other proteases may be involved and that post-translational modifications on Lys (either on APP or LRP8?) may represent a regulatory mechanism involved as well.

To further explore the involvement of other proteases in LICDs formation, we made an *in silico* analysis using MEROPS database (https://www.ebi.ac.uk/merops/), looking for proteases that may cleave the C-terminal portion of LRP8 after the γ-secretase site. This analysis gave a series of potential enzymes (**Figure 18**) which are involved also in APP processing and in the cleavage of other substrates of γ-secretase (see [39]).

By mean of qPCR experiments we have studied in SAD and control cases, in the same brain areas analyzed previously for LRP8, the expression of ADAM10, ADAM17, ADAMTS1, Cathepsin L, Cathepsin D, Meprin α and Meprin β. We

detected a significant increment of mRNA in SAD patients vs. controls only for ADAM10, ADAMTS1, Cathepsin D and Meprin β. Looking at the C-terminal sequence of LRP8 we determined that only ADAMTS1, Cathepsin D and Meprin β could be able to generate LICDs detected by our antibody GS1 (**Figure 18**); and, therefore, we decided to analyze by WB their level in the same samples previously analyzed by qPCR. The observation, at protein level, of the increment of these potentially active proteases in SAD samples (explanatory is the case of Cathepsin D), in comparison to controls, indicates that a transcriptional event, activated during AD, may contribute to the enhanced processing of LRP8, and likely of other substrates, in course of neurodegeneration. Previous works have shown, although in anecdotal manner, the elevated level of some proteases in AD brain [138,154]. However, these observations have always been referred to a potential role in APP cleavage or to the remodelling of the extracellular matrix in AD. In this case, we suggest a more specific role of selected proteases in the subsidiary cleavage of LRP8 when γ-secretase is hampered, therefore, linking their role to a parallel dysfunction of γ-secretase.

In conclusion, in this thesis we show that LRP8, a well-known receptor for ApoE involved in memory formation, is over-processed in course of AD and when γ-secretase is blocked. Its processing is likely mediated by other proteases, which are recruited when γ-secretase is genetically or pharmacologically hampered. The overall effect is characterized by a reduction of LRP8 holoprotein and a consequent increment of C-terminal fragments. Therefore, our finding corroborates the idea that, in case of a loss-of-function of PSENs, other substrates of γ-secretase, besides APP, undergo heavy changes, which could represent alternative diagnostic features of the disease. Whether these changes are either diagnostic or directly related to the etiology of the disease is yet to be determined. In this study we also confirm, and extend, previous anecdotal findings relative to an increased expression of selected endopeptidases in AD brains. The role of these enzymes may be relevant, either in consequence of their direct role in processing of signalling proteins such as LRP8 (as shown here) or, in general in force of their action in the remodelling of the extracellular matrix in the diseased brain.

BIBLIOGRAPHY

[1] L.E. Hebert, J. Weuve, P.A. Scherr, D.A. Evans, Alzheimer disease in the United States (2010-2050) estimated using the 2010 census, Neurology. 80 (2013) 1778–1783. doi:10.1212/WNL.0b013e31828726f5.

[2] American Psychiatric Association, Diagnostic and Statistical Manual of Mental Disorders, American Psychiatric Association, 2013. doi:10.1176/appi.books.9780890425596.

[3] A. Alzheimer, R.A. Stelzmann, H.N. Schnitzlein, F.R. Murtagh, An English translation of Alzheimer's 1907 paper, "Uber eine eigenartige Erkankung der Hirnrinde"., Clin. Anat. 8 (1995) 429–31. doi:10.1002/ca.980080612.

[4] G. McKhann, D. Drachman, M. Folstein, R. Katzman, D. Price, E.M. Stadlan, Clinical diagnosis of Alzheimer's disease: report of the NINCDS-ADRDA Work Group under the auspices of Department of Health and Human Services Task Force on Alzheimer's Disease., Neurology. 34 (1984) 939–44. http://www.ncbi.nlm.nih.gov/pubmed/6610841 (accessed February 15, 2018).

[5] G.G. Fillenbaum, G. van Belle, J.C. Morris, R.C. Mohs, S.S. Mirra, P.C. Davis, P.N. Tariot, J.M. Silverman, C.M. Clark, K.A. Welsh-Bohmer, A. Heyman, Consortium to Establish a Registry for Alzheimer's Disease (CERAD): the first twenty years., Alzheimers. Dement. 4 (2008) 96–109. doi:10.1016/j.jalz.2007.08.005.

[6] H. Braak, E. Braak, Staging of Alzheimer's disease-related neurofibrillary changes., Neurobiol. Aging. 16 (1995) 271-8-84. http://www.ncbi.nlm.nih.gov/pubmed/7566337.

[7] M. Goedert, Alzheimer's and Parkinson's diseases: The prion concept in relation to assembled Aβ, tau, and α-synuclein., Science. 349 (2015) 1255555. doi:10.1126/science.1255555.

[8] T.D. Bird, Genetic Factors in Alzheimer's Disease, N. Engl. J. Med. 352 (2005) 862–864. doi:10.1056/NEJMp058027.

[9] M. DiLuca, J. Olesen, The cost of brain diseases: a burden or a challenge?, Neuron. 82 (2014) 1205–8. doi:10.1016/j.neuron.2014.05.044.

[10] H. Zheng, E.H. Koo, The amyloid precursor protein: beyond amyloid., Mol. Neurodegener. 1 (2006) 5. doi:10.1186/1750-1326-1-5.

[11] S.S. Sisodia, E.H. Koo, P.N. Hoffman, G. Perry, D.L. Price, Identification and transport of full-length amyloid precursor proteins in rat peripheral nervous system., J. Neurosci. 13 (1993) 3136–42. http://www.ncbi.nlm.nih.gov/pubmed/8331390.

[12] T. Matsui, M. Ingelsson, H. Fukumoto, K. Ramasamy, H. Kowa, M.P. Frosch, M.C. Irizarry, B.T. Hyman, Expression of APP pathway mRNAs and proteins in Alzheimer's disease, Brain Res. 1161 (2007) 116–123. doi:10.1016/j.brainres.2007.05.050.

[13] T.M.J. Allinson, E.T. Parkin, A.J. Turner, N.M. Hooper, ADAMs family members as amyloid precursor protein γ-secretases, J. Neurosci. Res. 74 (2003) 342–352. doi:10.1002/jnr.10737.

[14] R. Vassar, B.D. Bennett, S. Babu-Khan, S. Kahn, E.A. Mendiaz, P. Denis, D.B. Teplow, S. Ross, P. Amarante, R. Loeloff, Y. Luo, S. Fisher, J. Fuller, S. Edenson, J. Lile, M.A. Jarosinski, A.L. Biere, E. Curran, T. Burgess, J.C. Louis, F. Collins, J. Treanor, G. Rogers, M. Citron, Beta-secretase cleavage of Alzheimer's amyloid precursor protein by the transmembrane aspartic protease BACE., Science. 286 (1999) 735–41. http://www.ncbi.nlm.nih.gov/pubmed/10531052.

[15] R. Yan, M.J. Bienkowski, M.E. Shuck, H. Miao, M.C. Tory, A.M. Pauley, J.R. Brashler, N.C. Stratman, W.R. Mathews, A.E. Buhl, D.B. Carter, A.G. Tomasselli, L.A. Parodi, R.L. Heinrikson, M.E. Gurney, Membrane-anchored aspartyl protease with Alzheimer's disease β-secretase activity, Nature. 402 (1999) 533–537. doi:10.1038/990107.

[16] M.S. Wolfe, R. Kopan, Intramembrane proteolysis: theme and variations., Science. 305 (2004) 1119–23. doi:10.1126/science.1096187.

[17] J.O. Ebinu, B.A. Yankner, A RIP tide in neuronal signal transduction., Neuron. 34 (2002) 499–502. http://www.ncbi.nlm.nih.gov/pubmed/12062033.

[18] C. Beckett, N.N. Nalivaeva, N.D. Belyaev, A.J. Turner, Nuclear signalling by membrane protein intracellular domains: the AICD enigma, Cell. Signal. 24 (2012) 402–409. doi:10.1016/j.cellsig.2011.10.007.

[19] B. De Strooper, R. Vassar, T. Golde, The secretases: enzymes with therapeutic potential in Alzheimer disease, Nat. Rev. Neurol. 6 (2010) 99–107. doi:10.1038/nrneurol.2009.218.

[20] M. Tabaton, P. Gambetti, Soluble amyloid-beta in the brain: the scarlet pimpernel, J. Alzheimer's Dis. JAD. 9 (2006) 127–132.

[21] J.K. Teller, C. Russo, L.M. DeBusk, G. Angelini, D. Zaccheo, F. Dagna-Bricarelli, P. Scartezzini, S. Bertolini, D.M. Mann, M. Tabaton, P. Gambetti, Presence of soluble amyloid beta-peptide precedes amyloid plaque formation in Down's syndrome, Nat. Med. 2 (1996) 93–95.

[22] D.J. Selkoe, J. Hardy, The amyloid hypothesis of Alzheimer's disease at 25 years, EMBO Mol. Med. 8 (2016) 595–608. doi:10.15252/emmm.201606210.

[23] J.A. Hardy, G.A. Higgins, Alzheimer's disease: the amyloid cascade hypothesis., Science. 256 (1992) 184–5. http://www.ncbi.nlm.nih.gov/pubmed/1566067.

[24] J. Hardy, D.J. Selkoe, The Amyloid Hypothesis of Alzheimer's Disease: Progress and Problems on the Road to Therapeutics, Science (80-.). 297 (2002) 353–356. doi:10.1126/science.1072994.

[25] A. Rapp, B. Gmeiner, M. Hüttinger, Implication of apoE isoforms in cholesterol metabolism by primary rat hippocampal neurons and astrocytes, Biochimie. 88 (2006) 473–483. doi:10.1016/j.biochi.2005.10.007.

[26] S. Aleshkov, C.R. Abraham, V.I. Zannis, Interaction of Nascent ApoE2, ApoE3, and ApoE4 Isoforms Expressed in Mammalian Cells with Amyloid Peptide β (1−40). Relevance to Alzheimer's Disease., Biochemistry. 36 (1997) 10571–10580. doi:10.1021/bi9626362.

[27] J. Petrlova, H.-S. Hong, D.A. Bricarello, G. Harishchandra, G.A. Lorigan, L.-W. Jin, J.C. Voss, A differential association of Apolipoprotein E isoforms with the amyloid-β oligomer in solution, Proteins Struct. Funct. Bioinforma. 79 (2011) 402–416. doi:10.1002/prot.22891.

[28] K.R. Bales, T. Verina, R.C. Dodel, Y. Du, L. Altstiel, M. Bender, P. Hyslop, E.M. Johnstone, S.P. Little, D.J. Cummins, P. Piccardo, B. Ghetti, S.M. Paul, Lack of apolipoprotein E dramatically reduces amyloid beta-peptide deposition., Nat. Genet. 17 (1997) 263–4. doi:10.1038/ng1197-263.

[29] M.C. Irizarry, G.W. Rebeck, B. Cheung, K. Bales, S.M. Paul, D. Holzman, B.T. Hyman, Modulation of A beta deposition in APP transgenic mice by an apolipoprotein E null background., Ann. N. Y. Acad. Sci. 920 (2000) 171–8. http://www.ncbi.nlm.nih.gov/pubmed/11193147.

[30] B. De Strooper, L. Chávez Gutiérrez, Learning by failing: ideas and concepts to tackle γ-secretases in Alzheimer's disease and beyond, Annu. Rev. Pharmacol. Toxicol. 55 (2015) 419–437. doi:10.1146/annurev-pharmtox-010814-124309.

[31] W.T. Kimberly, M.J. LaVoie, B.L. Ostaszewski, W. Ye, M.S. Wolfe, D.J. Selkoe, Gamma-secretase is a membrane protein complex comprised of presenilin, nicastrin, Aph-1, and Pen-2., Proc. Natl. Acad. Sci. U. S. A. 100 (2003) 6382–7. doi:10.1073/pnas.1037392100.

[32] P. St George-Hyslop, G. Yu, M. Nishimura, S. Arawaka, D. Levitan, L. Zhang, A. Tandon, Y.-Q. Song, E. Rogaeva, F. Chen, T. Kawarai, A. Supala, L. Levesque, H. Yu, D.-S. Yang, E. Holmes, P. Milman, Y. Liang, D.M. Zhang, D.H. Xu, C. Sato, E. Rogaev, M. Smith, C. Janus, Y. Zhang, R. Aebersold, L. Farrer, S. Sorbi, A. Bruni, P. Fraser, Nicastrin modulates presenilin-mediated notch/glp-1 signal transduction and betaAPP processing., Nature. 407 (2000) 48–54. doi:10.1038/35024009.

[33] C.B. Lessard, B.A. Cottrell, H. Maruyama, S. Suresh, T.E. Golde, E.H. Koo, γ-Secretase Modulators and APH1 Isoforms Modulate γ-Secretase Cleavage but Not Position of ε-Cleavage of the Amyloid Precursor Protein (APP)., PLoS One. 10 (2015) e0144758. doi:10.1371/journal.pone.0144758.

[34] B. De Strooper, Aph-1, Pen-2, and Nicastrin with Presenilin generate an active gamma-Secretase complex., Neuron. 38 (2003) 9–12. http://www.ncbi.nlm.nih.gov/pubmed/12691659.

[35] M.B. Podlisny, M. Citron, P. Amarante, R. Sherrington, W. Xia, J. Zhang, T. Diehl, G. Levesque, P. Fraser, C. Haass, E.H. Koo, P. Seubert, P. St George-Hyslop, D.B. Teplow, D.J. Selkoe, Presenilin proteins undergo heterogeneous endoproteolysis between Thr291 and Ala299 and occur as stable N- and C-terminal fragments in normal and Alzheimer brain tissue., Neurobiol. Dis. 3 (1997) 325–37. doi:10.1006/nbdi.1997.0129.

[36] G. Thinakaran, D.R. Borchelt, M.K. Lee, H.H. Slunt, L. Spitzer, G. Kim, T. Ratovitsky, F. Davenport, C. Nordstedt, M. Seeger, J. Hardy, A.I. Levey, S.E. Gandy, N.A. Jenkins, N.G. Copeland, D.L. Price, S.S. Sisodia, Endoproteolysis of presenilin 1 and accumulation of processed derivatives in vivo., Neuron. 17 (1996) 181–90. http://www.ncbi.nlm.nih.gov/pubmed/8755489 (accessed March 28, 2017).

[37] C. Sato, Y. Morohashi, T. Tomita, T. Iwatsubo, Structure of the catalytic pore of gamma-secretase probed by the accessibility of substituted cysteines, J. Neurosci. 26 (2006) 12081–12088. doi:10.1523/JNEUROSCI.3614-06.2006.

[38] A. Haapasalo, D.M. Kovacs, The many substrates of presenilin/γ-secretase, J. Alzheimer's Dis. JAD. 25 (2011) 3–28. doi:10.3233/JAD-2011-101065.

[39] A. Medoro, S. Bartollino, D. Mignogna, D. Passarella, C. Porcile, A. Pagano, T. Florio, M. Nizzari, G. Guerra, R. Di Marco, M. Intrieri, G. Raimo, C. Russo, Complexity and Selectivity of γ-Secretase Cleavage on Multiple Substrates: Consequences in Alzheimer's Disease and Cancer, J. Alzheimer's Dis. 61 (2018) 1–15. doi:10.3233/JAD-170628.

[40] R. Sherrington, E.I. Rogaev, Y. Liang, E.A. Rogaeva, G. Levesque, M. Ikeda, H. Chi, C. Lin, G. Li, K. Holman, T. Tsuda, L. Mar, J.-F. Foncin, A.C. Bruni, M.P. Montesi, S. Sorbi, I. Rainero, L.

Pinessi, L. Nee, I. Chumakov, D. Pollen, A. Brookes, P. Sanseau, R.J. Polinsky, W. Wasco, H.A.R. Da Silva, J.L. Haines, M.A. Pericak-Vance, R.E. Tanzi, A.D. Roses, P.E. Fraser, J.M. Rommens, P.H. St George-Hyslop, Cloning of a gene bearing missense mutations in early-onset familial Alzheimer's disease, Nature. 375 (1995) 754–760. doi:10.1038/375754a0.

[41] E.I. Rogaev, R. Sherrington, E.A. Rogaeva, G. Levesque, M. Ikeda, Y. Liang, H. Chi, C. Lin, K. Holman, T. Tsuda, L. Mar, S. Sorbi, B. Nacmias, S. Piacentini, L. Amaducci, I. Chumakov, D. Cohen, L. Lannfelt, P.E. Fraser, J.M. Rommens, P.H.S. George-Hyslop, Familial Alzheimer's disease in kindreds with missense mutations in a gene on chromosome 1 related to the Alzheimer's disease type 3 gene, Nature. 376 (1995) 775–778. doi:10.1038/376775a0.

[42] C. Van Cauwenberghe, C. Van Broeckhoven, K. Sleegers, The genetic landscape of Alzheimer disease: clinical implications and perspectives, Genet. Med. Off. J. Am. Coll. Med. Genet. 18 (2016) 421–430. doi:10.1038/gim.2015.117.

[43] M.A. Fernandez, J.A. Klutkowski, T. Freret, M.S. Wolfe, Alzheimer presenilin-1 mutations dramatically reduce trimming of long amyloid β-peptides (Aβ) by γ-secretase to increase 42-to-40-residue Aβ., J. Biol. Chem. 289 (2014) 31043–52. doi:10.1074/jbc.M114.581165.

[44] J. Shen, Function and dysfunction of presenilin, Neurodegener. Dis. 13 (2014) 61–63. doi:10.1159/000354971.

[45] J. Shen, R.J. Kelleher, The presenilin hypothesis of Alzheimer's disease: evidence for a loss-of-function pathogenic mechanism, Proc. Natl. Acad. Sci. U. S. A. 104 (2007) 403–409. doi:10.1073/pnas.0608332104.

[46] Q. Chen, A. Nakajima, S.H. Choi, X. Xiong, Y.-P. Tang, Loss of presenilin function causes Alzheimer's disease-like neurodegeneration in the mouse, J. Neurosci. Res. 86 (2008) 1615–1625. doi:10.1002/jnr.21601.

[47] C.A. Saura, S. Choi, V. Beglopoulos, S. Malkani, D. Zhang, B.S.S. Rao, S. Chattarji, R.J.K. Iii, E.R. Kandel, K. Duff, A. Kirkwood, J. Shen, Loss of Presenilin Function Causes Impairments of Memory and Synaptic Plasticity Followed by Age-Dependent Neurodegeneration, 42 (2004) 23–36.

[48] C. Russo, G. Schettini, T.C. Saido, C. Hulette, C. Lippa, L. Lannfelt, B. Ghetti, P. Gambetti, M. Tabaton, J.K. Teller, Presenilin-1 mutations in Alzheimer's disease, Nature. 405 (2000) 531–532. doi:10.1038/35014735.

[49] C. Russo, E. Violani, S. Salis, V. Venezia, V. Dolcini, G. Damonte, U. Benatti, C. D'Arrigo, E. Patrone, P. Carlo, G. Schettini, Pyroglutamate-modified amyloid beta-peptides--AbetaN3(pE)--strongly affect cultured neuron and astrocyte survival, J. Neurochem. 82 (2002) 1480–1489.

[50] R. Ma, Y. Zhang, X. Hong, J. Zhang, J.-Z. Wang, G. Liu, Role of microtubule-associated protein tau phosphorylation in Alzheimer's disease, J. Huazhong Univ. Sci. Technol. [Medical Sci. 37 (2017) 307–312. doi:10.1007/s11596-017-1732-x.

[51] C. Ballatore, V.M.-Y. Lee, J.Q. Trojanowski, Tau-mediated neurodegeneration in Alzheimer's disease and related disorders, Nat. Rev. Neurosci. 8 (2007) 663–672. doi:10.1038/nrn2194.

[52] F.P. Chong, K.Y. Ng, R.Y. Koh, S.M. Chye, Tau Proteins and Tauopathies in Alzheimer's Disease, Cell. Mol. Neurobiol. (2018). doi:10.1007/s10571-017-0574-1.

[53] R.B. Maccioni, G. Farías, I. Morales, L. Navarrete, The Revitalized Tau Hypothesis on Alzheimer's Disease, Arch. Med. Res. 41 (2010) 226–231. doi:10.1016/j.arcmed.2010.03.007.

[54] A.H. Moore, M.K. O'Banion, Neuroinflammation and anti-inflammatory therapy for Alzheimer's disease., Adv. Drug Deliv. Rev. 54 (2002) 1627–56. http://www.ncbi.nlm.nih.gov/pubmed/12453679.

[55] E.E. Tuppo, H.R. Arias, The role of inflammation in Alzheimer's disease., Int. J. Biochem. Cell Biol. 37 (2005) 289–305. doi:10.1016/j.biocel.2004.07.009.

[56] H. Lum, K.A. Roebuck, Oxidant stress and endothelial cell dysfunction, Am. J. Physiol. Physiol. 280 (2001) C719–C741. doi:10.1152/ajpcell.2001.280.4.C719.

[57] G. Aliev, M.A. Smith, D. Seyidov, M.L. Neal, B.T. Lamb, A. Nunomura, E.K. Gasimov, H. V Vinters, G. Perry, J.C. LaManna, R.P. Friedland, The role of oxidative stress in the pathophysiology of cerebrovascular lesions in Alzheimer's disease., Brain Pathol. 12 (2002) 21–35. http://www.ncbi.nlm.nih.gov/pubmed/11770899.

[58] X. Zhu, S.L. Siedlak, Y. Wang, G. Perry, R.J. Castellani, M.L. Cohen, M.A. Smith, Neuronal binucleation in Alzheimer disease hippocampus., Neuropathol. Appl. Neurobiol. 34 (2008) 457–65. doi:10.1111/j.1365-2990.2007.00908.x.

[59] K.H.J. Park, J.L. Hallows, P. Chakrabarty, P. Davies, I. Vincent, Conditional neuronal simian virus 40 T antigen expression induces Alzheimer-like tau and amyloid pathology in mice., J. Neurosci. 27 (2007) 2969–78. doi:10.1523/JNEUROSCI.0186-07.2007.

[60] I. Vincent, J.H. Zheng, D.W. Dickson, Y. Kress, P. Davies, Mitotic phosphoepitopes precede paired helical filaments in Alzheimer's disease., Neurobiol. Aging. 19 (n.d.) 287–96. http://www.ncbi.nlm.nih.gov/pubmed/9733160.

[61] R.L. Neve, D.L. McPhie, Dysfunction of amyloid precursor protein signaling in neurons leads to DNA synthesis and apoptosis, Biochim. Biophys. Acta. 1772 (2007) 430–437. doi:10.1016/j.bbadis.2006.10.008.

[62] D. Langosch, H. Steiner, Substrate processing in intramembrane proteolysis by ?-secretase ? the role of protein dynamics, Biol. Chem. 398 (2017) 441–453. doi:10.1515/hsz-2016-0269.

[63] D.B. Donoviel, A.K. Hadjantonakis, M. Ikeda, H. Zheng, P.S. Hyslop, A. Bernstein, Mice lacking both presenilin genes exhibit early embryonic patterning defects., Genes Dev. 13 (1999) 2801–10. http://www.ncbi.nlm.nih.gov/pubmed/10557208.

[64] R.S. Doody, R. Raman, M. Farlow, T. Iwatsubo, B. Vellas, S. Joffe, K. Kieburtz, F. He, X. Sun, R.G. Thomas, P.S. Aisen, E. Siemers, G. Sethuraman, R. Mohs, R. Mohs, Semagacestat Study Group, A Phase 3 Trial of Semagacestat for Treatment of Alzheimer's Disease, N. Engl. J. Med. 369 (2013) 341–350. doi:10.1056/NEJMoa1210951.

[65] L. Chávez-Gutiérrez, L. Bammens, I. Benilova, A. Vandersteen, M. Benurwar, M. Borgers, S. Lismont, L. Zhou, S. Van Cleynenbreugel, H. Esselmann, J. Wiltfang, L. Serneels, E. Karran, H. Gijsen, J. Schymkowitz, F. Rousseau, K. Broersen, B. De Strooper, The mechanism of γ-Secretase dysfunction in familial Alzheimer disease, EMBO J. 31 (2012) 2261–2274. doi:10.1038/emboj.2012.79.

[66] C. Niva, J. Parkinson, F. Olsson, E. van Schaick, J. Lundkvist, S.A.G. Visser, Has inhibition of

Aβ production adequately been tested as therapeutic approach in mild AD? A model-based meta-analysis of γ-secretase inhibitor data., Eur. J. Clin. Pharmacol. 69 (2013) 1247–60. doi:10.1007/s00228-012-1459-3.

[67] B. De Strooper, Lessons from a failed γ-secretase Alzheimer trial, Cell. 159 (2014) 721–726. doi:10.1016/j.cell.2014.10.016.

[68] L. Bammens, L. Chávez-Gutiérrez, A. Tolia, A. Zwijsen, B. De Strooper, Functional and topological analysis of Pen-2, the fourth subunit of the gamma-secretase complex, J. Biol. Chem. 286 (2011) 12271–82. doi:10.1074/jbc.M110.216978.

[69] T. Li, G. Ma, H. Cai, D.L. Price, P.C. Wong, Nicastrin is required for assembly of presenilin/gamma-secretase complexes to mediate Notch signaling and for processing and trafficking of beta-amyloid precursor protein in mammals., 23 (2003) 3272–3277.

[70] J. Shen, R.T. Bronson, D.F. Chen, W. Xia, D.J. Selkoe, S. Tonegawa, Skeletal and CNS Defects in Presenilin-1 -Deficient Mice, 89 (1997) 629–639. doi:10.1016/S0030-6657(08)70226-9.

[71] D.B. Henley, K.L. Sundell, G. Sethuraman, S.A. Dowsett, P.C. May, Safety profile of semagacestat, a gamma-secretase inhibitor: IDENTITY trial findings., Curr. Med. Res. Opin. 30 (2014) 2021–32. doi:10.1185/03007995.2014.939167.

[72] C.J. Crump, S. V Castro, F. Wang, N. Pozdnyakov, T.E. Ballard, S.S. Sisodia, K.R. Bales, D.S. Johnson, Y. Li, BMS-708,163 Targets Presenilin and Lacks Notch-Sparing Activity, (2012) 7209–7211. doi:10.1021/bi301137h.

[73] B. De Craene, G. Berx, Regulatory networks defining EMT during cancer initiation and progression, Nat. Rev. Cancer. 13 (2013) 97–110. doi:10.1038/nrc3447.

[74] D.M. Holtzman, J. Herz, G. Bu, Apolipoprotein E and apolipoprotein E receptors: normal biology and roles in Alzheimer disease., Cold Spring Harb. Perspect. Med. 2 (2012) a006312. doi:10.1101/cshperspect.a006312.

[75] M.J. LaDu, G.W. Munson, L. Jungbauer, G.S. Getz, C.A. Reardon, L.M. Tai, C. Yu, Preferential interactions between ApoE-containing lipoproteins and Aβ revealed by a detection method that combines size exclusion chromatography with non-reducing gel-shift, Biochim. Biophys. Acta. 1821 (2012) 295–302. doi:10.1016/j.bbalip.2011.11.005.

[76] C. Russo, G. Angelini, D. Dapino, A. Piccini, G. Piombo, G. Schettini, S. Chen, J.K. Teller, D. Zaccheo, P. Gambetti, M. Tabaton, Opposite roles of apolipoprotein E in normal brains and in Alzheimer's disease, Proc. Natl. Acad. Sci. U. S. A. 95 (1998) 15598–15602.

[77] L.M. Tai, T. Bilousova, L. Jungbauer, S.K. Roeske, K.L. Youmans, C. Yu, W.W. Poon, L.B. Cornwell, C.A. Miller, H. V. Vinters, L.J. Van Eldik, D.W. Fardo, S. Estus, G. Bu, K.H. Gylys, M.J. Ladu, Levels of soluble apolipoprotein E/amyloid-β (Aβ) complex are reduced and oligomeric Aβ increased with APOE4 and Alzheimer disease in a transgenic mouse model and human samples, J. Biol. Chem. 288 (2013) 5914–5926. doi:10.1074/jbc.M112.442103.

[78] A.B. Wolf, J. Valla, G. Bu, J. Kim, M.J. LaDu, E.M. Reiman, R.J. Caselli, Apolipoprotein E as a β-amyloid-independent factor in Alzheimer's disease, Alzheimers. Res. Ther. 5 (2013) 38. doi:10.1186/alzrt204.

[79] Y. Chen, M.S. Durakoglugil, X. Xian, J. Herz, ApoE4 reduces glutamate receptor function and synaptic plasticity by selectively impairing ApoE receptor recycling, Proc. Natl. Acad. Sci. U. S. A. 107 (2010) 12011–12016. doi:10.1073/pnas.0914984107.

[80] S.B. Dumanis, A.M. DiBattista, M. Miessau, C.E.H. Moussa, G.W. Rebeck, APOE genotype affects the pre-synaptic compartment of glutamatergic nerve terminals, J. Neurochem. 124 (2013) 4–14. doi:10.1111/j.1471-4159.2012.07908.x.

[81] H.-S. Hoe, G.W. Rebeck, Functional interactions of APP with the apoE receptor family, J. Neurochem. 106 (2008) 2263–2271. doi:10.1111/j.1471-4159.2008.05517.x.

[82] Y. Motoi, M. Itaya, H. Mori, Y. Mizuno, T. Iwasaki, H. Hattori, S. Haga, K. Ikeda, Apolipoprotein E receptor 2 is involved in neuritic plaque formation in APP sw mice., Neurosci. Lett. 368 (2004) 144–7. doi:10.1016/j.neulet.2004.06.081.

[83] T. Kanekiyo, C.-C. Liu, M. Shinohara, J. Li, G. Bu, LRP1 in brain vascular smooth muscle cells mediates local clearance of Alzheimer's amyloid-β, J. Neurosci. Off. J. Soc. Neurosci. 32 (2012) 16458–16465. doi:10.1523/JNEUROSCI.3987-12.2012.

[84] T. Pflanzner, M.C. Janko, B. André-Dohmen, S. Reuss, S. Weggen, A.J.M. Roebroek, C.R.W. Kuhlmann, C.U. Pietrzik, LRP1 mediates bidirectional transcytosis of amyloid-β across the blood-brain barrier, Neurobiol. Aging. 32 (2011) 2323.e1-11. doi:10.1016/j.neurobiolaging.2010.05.025.

[85] R. Deane, A. Sagare, K. Hamm, M. Parisi, S. Lane, M.B. Finn, D.M. Holtzman, B. V. Zlokovic, apoE isoform-specific disruption of amyloid beta peptide clearance from mouse brain, J. Clin. Invest. 118 (2008) 4002–4013. doi:10.1172/JCI36663.

[86] R.A. Fuentealba, M.I. Barría, J. Lee, J. Cam, C. Araya, C.A. Escudero, N.C. Inestrosa, F.C. Bronfman, G. Bu, M.-P. Marzolo, ApoER2 expression increases Abeta production while decreasing Amyloid Precursor Protein (APP) endocytosis: Possible role in the partitioning of APP into lipid rafts and in the regulation of gamma-secretase activity, Mol. Neurodegener. 2 (2007) 14. doi:10.1186/1750-1326-2-14.

[87] A.M. DiBattista, S.B. Dumanis, J.M. Song, G. Bu, E. Weeber, G. William Rebeck, H.-S. Hoe, Very low density lipoprotein receptor regulates dendritic spine formation in a RasGRF1/CaMKII dependent manner, Biochim. Biophys. Acta - Mol. Cell Res. 1853 (2015) 904–917. doi:10.1016/j.bbamcr.2015.01.015.

[88] M. Trommsdorff, M. Gotthardt, T. Hiesberger, J. Shelton, W. Stockinger, J. Nimpf, R.E. Hammer, J.A. Richardson, J. Herz, Reeler/Disabled-like disruption of neuronal migration in knockout mice lacking the VLDL receptor and ApoE receptor 2., Cell. 97 (1999) 689–701. http://www.ncbi.nlm.nih.gov/pubmed/10380922.

[89] S. Hellwig, I. Hack, B. Zucker, B. Brunne, D. Junghans, Reelin together with ApoER2 regulates interneuron migration in the olfactory bulb, PLoS One. 7 (2012) e50646. doi:10.1371/journal.pone.0050646.

[90] V. Strasser, D. Fasching, C. Hauser, H. Mayer, H.H. Bock, T. Hiesberger, J. Herz, E.J. Weeber, J.D. Sweatt, A. Pramatarova, B. Howell, W.J. Schneider, J. Nimpf, Receptor clustering is involved in Reelin signaling., Mol. Cell. Biol. 24 (2004) 1378–86. http://www.ncbi.nlm.nih.gov/pubmed/14729980.

[91] H.-S. Hoe, T.S. Tran, Y. Matsuoka, B.W. Howell, G.W. Rebeck, DAB1 and Reelin effects on amyloid precursor protein and ApoE receptor 2 trafficking and processing, J. Biol. Chem. 281 (2006) 35176–35185. doi:10.1074/jbc.M602162200.

[92] Y. Hirota, K. Kubo, T. Fujino, T.T. Yamamoto, K. Nakajima, ApoER2 Controls Not Only Neuronal Migration in the Intermediate Zone But Also Termination of Migration in the Developing Cerebral Cortex, Cereb. Cortex. 28 (2018) 223–235. doi:10.1093/cercor/bhw369.

[93] G. D'Arcangelo, R. Homayouni, L. Keshvara, D.S. Rice, M. Sheldon, T. Curran, Reelin is a ligand for lipoprotein receptors., Neuron. 24 (1999) 471–9. http://www.ncbi.nlm.nih.gov/pubmed/10571240.

[94] J. Herz, U. Beffert, Apolipoprotein E receptors: linking brain development and Alzheimer's disease., Nat. Rev. Neurosci. 1 (2000) 51–8. doi:10.1038/35036221.

[95] T.L. Young-Pearse, J. Bai, R. Chang, J.B. Zheng, J.J. LoTurco, D.J. Selkoe, A critical function for beta-amyloid precursor protein in neuronal migration revealed by in utero RNA interference, J. Neurosci. 27 (2007) 14459–14469. doi:10.1523/JNEUROSCI.4701-07.2007.

[96] D.G. Callahan, W.M. Taylor, M. Tilearcio, T. Cavanaugh, D.J. Selkoe, T.L. Young-Pearse, Embryonic mosaic deletion of APP results in displaced Reelin-expressing cells in the cerebral cortex, Dev. Biol. 424 (2017) 138–146. doi:10.1016/j.ydbio.2017.03.007.

[97] A. Ho, T.C. Südhof, Binding of F-spondin to amyloid-beta precursor protein: a candidate amyloid-beta precursor protein ligand that modulates amyloid-beta precursor protein cleavage., Proc. Natl. Acad. Sci. U. S. A. 101 (2004) 2548–53. http://www.ncbi.nlm.nih.gov/pubmed/14983046.

[98] H.-S. Hoe, D. Wessner, U. Beffert, A.G. Becker, Y. Matsuoka, G.W. Rebeck, F-spondin interaction with the apolipoprotein E receptor ApoEr2 affects processing of amyloid precursor protein., Mol. Cell. Biol. 25 (2005) 9259–68. doi:10.1128/MCB.25.21.9259-9268.2005.

[99] C.U. Pietrzik, I.-S. Yoon, S. Jaeger, T. Busse, S. Weggen, E.H. Koo, FE65 constitutes the functional link between the low-density lipoprotein receptor-related protein and the amyloid precursor protein., J. Neurosci. 24 (2004) 4259–65. doi:10.1523/JNEUROSCI.5451-03.2004.

[100] C.U. Pietrzik, T. Busse, D.E. Merriam, S. Weggen, E.H. Koo, The cytoplasmic domain of the LDL receptor-related protein regulates multiple steps in APP processing., EMBO J. 21 (2002) 5691–700. http://www.ncbi.nlm.nih.gov/pubmed/12411487.

[101] G. Minopoli, M. Stante, F. Napolitano, F. Telese, L. Aloia, M. De Felice, R. Di Lauro, R. Pacelli, A. Brunetti, N. Zambrano, T. Russo, Essential roles for Fe65, Alzheimer amyloid precursor-binding protein, in the cellular response to DNA damage, J. Biol. Chem. 282 (2007) 831–835. doi:10.1074/jbc.C600276200.

[102] M. Stante, G. Minopoli, F. Passaro, M. Raia, L. Del Vecchio, T. Russo, Fe65 is required for Tip60-directed histone H4 acetylation at DNA strand breaks, Proc. Natl. Acad. Sci. U. S. A. 106 (2009) 5093–5098. doi:10.1073/pnas.0810869106.

[103] S.C. Domingues, U. Konietzko, A.G. Henriques, S. Rebelo, M. Fardilha, H. Nishitani, R.M. Nitsch, E.F. da Cruz E Silva, O.A.B. da Cruz E Silva, RanBP9 modulates AICD localization and transcriptional activity via direct interaction with Tip60, J. Alzheimer's Dis. JAD. 42 (2014) 1415–1433. doi:10.3233/JAD-132495.

[104] F. Telese, Q. Ma, P.M. Perez, D. Notani, S. Oh, W. Li, D. Comoletti, K.A. Ohgi, H. Taylor, M.G. Rosenfeld, LRP8-Reelin-Regulated Neuronal Enhancer Signature Underlying Learning and Memory Formation, Neuron. 86 (2015) 696–710. doi:10.1016/j.neuron.2015.03.033.

[105] Q. Liu, C. V. Zerbinatti, J. Zhang, H.-S. Hoe, B. Wang, S.L. Cole, J. Herz, L. Muglia, G. Bu, Amyloid precursor protein regulates brain apolipoprotein E and cholesterol metabolism through lipoprotein receptor LRP1, Neuron. 56 (2007) 66–78. doi:10.1016/j.neuron.2007.08.008.

[106] U. Beffert, E.J. Weeber, A. Durudas, S. Qiu, I. Masiulis, J.D. Sweatt, W.-P. Li, G. Adelmann, M. Frotscher, R.E. Hammer, J. Herz, Modulation of synaptic plasticity and memory by Reelin involves differential splicing of the lipoprotein receptor Apoer2., Neuron. 47 (2005) 567–79. doi:10.1016/j.neuron.2005.07.007.

[107] H.-S. Hoe, A. Pocivavsek, G. Chakraborty, Z. Fu, S. Vicini, M.D. Ehlers, G.W. Rebeck, Apolipoprotein E Receptor 2 Interactions with the *N* -Methyl-D-aspartate Receptor, J. Biol. Chem. 281 (2006) 3425–3431. doi:10.1074/jbc.M509380200.

[108] E. Ampuero, N. Jury, S. Härtel, M.-P. Marzolo, B. van Zundert, Interfering of the Reelin/ApoER2/PSD95 Signaling Axis Reactivates Dendritogenesis of Mature Hippocampal Neurons., J. Cell. Physiol. 232 (2017) 1187–1199. doi:10.1002/jcp.25605.

[109] C. Nakajima, A. Kulik, M. Frotscher, J. Herz, M. Schäfer, H.H. Bock, P. May, Low density lipoprotein receptor-related protein 1 (LRP1) modulates N-methyl-D-aspartate (NMDA) receptor-dependent intracellular signaling and NMDA-induced regulation of postsynaptic protein complexes, J. Biol. Chem. 288 (2013) 21909–21923. doi:10.1074/jbc.M112.444364.

[110] V. Balmaceda, I. Cuchillo-Ibáñez, L. Pujadas, M.-S. García-Ayllón, C.A. Saura, J. Nimpf, E. Soriano, J. Sáez-Valero, ApoER2 processing by presenilin-1 modulates reelin expression, FASEB J. Off. Publ. Fed. Am. Soc. Exp. Biol. 28 (2014) 1543–1554. doi:10.1096/fj.13-239350.

[111] R. De Gasperi, M.A. Gama Sosa, P.H. Wen, J. Li, G.M. Perez, T. Curran, G.A. Elder, Cortical development in the presenilin-1 null mutant mouse fails after splitting of the preplate and is not due to a failure of reelin-dependent signaling, Dev. Dyn. An Off. Publ. Am. Assoc. Anat. 237 (2008) 2405–2414. doi:10.1002/dvdy.21661.

[112] W. Wang, A.M. Moerman-Herzog, A. Slaton, S.W. Barger, Presenilin 1 mutations influence processing and trafficking of the ApoE receptor apoER2., Neurobiol. Aging. 49 (2017) 145–153. doi:10.1016/j.neurobiolaging.2016.10.005.

[113] C. Lane-Donovan, J. Herz, The ApoE receptors Vldlr and Apoer2 in central nervous system function and disease, J. Lipid Res. 58 (2017) 1036–1043. doi:10.1194/jlr.R075507.

[114] S.S. Reddy, T.E. Connor, E.J. Weeber, W. Rebeck, Similarities and differences in structure, expression, and functions of VLDLR and ApoER2, Mol. Neurodegener. 6 (2011) 30. doi:10.1186/1750-1326-6-30.

[115] J. Su, M.A. Klemm, A.M. Josephson, M.A. Fox, Contributions of VLDLR and LRP8 in the establishment of retinogeniculate projections, Neural Dev. 8 (2013) 11. doi:10.1186/1749-8104-8-11.

[116] S. Massone, E. Ciarlo, S. Vella, M. Nizzari, T. Florio, C. Russo, R. Cancedda, A. Pagano, NDM29, a RNA polymerase III-dependent non coding RNA, promotes amyloidogenic processing of APP and amyloid β secretion., Biochim. Biophys. Acta. 1823 (2012) 1170–7.

doi:10.1016/j.bbamcr.2012.05.001.

[117] G. Corso, A. Cristofano, N. Sapere, G. la Marca, A. Angiolillo, M. Vitale, R. Fratangelo, T. Lombardi, C. Porcile, M. Intrieri, A. Di Costanzo, Serum Amino Acid Profiles in Normal Subjects and in Patients with or at Risk of Alzheimer Dementia, Dement. Geriatr. Cogn. Dis. Extra. 7 (2017) 143–159. doi:10.1159/000466688.

[118] G.M. McKhann, D.S. Knopman, H. Chertkow, B.T. Hyman, C.R. Jack, C.H. Kawas, W.E. Klunk, W.J. Koroshetz, J.J. Manly, R. Mayeux, R.C. Mohs, J.C. Morris, M.N. Rossor, P. Scheltens, M.C. Carrillo, B. Thies, S. Weintraub, C.H. Phelps, The diagnosis of dementia due to Alzheimer's disease: recommendations from the National Institute on Aging-Alzheimer's Association workgroups on diagnostic guidelines for Alzheimer's disease., Alzheimers. Dement. 7 (2011) 263–9. doi:10.1016/j.jalz.2011.03.005.

[119] M.S. Albert, S.T. DeKosky, D. Dickson, B. Dubois, H.H. Feldman, N.C. Fox, A. Gamst, D.M. Holtzman, W.J. Jagust, R.C. Petersen, P.J. Snyder, M.C. Carrillo, B. Thies, C.H. Phelps, The diagnosis of mild cognitive impairment due to Alzheimer's disease: recommendations from the National Institute on Aging-Alzheimer's Association workgroups on diagnostic guidelines for Alzheimer's disease., Alzheimers. Dement. 7 (2011) 270–9. doi:10.1016/j.jalz.2011.03.008.

[120] G. Spinnler, H; Tognoni, Italian standardization and classification of Neuropsychological tests. The Italian Group on the Neuropsychological Study of Aging., Ital. J. Neurol. Sci. Suppl 8 (1987) 1–120.

[121] I. Penna, S. Vella, A. Gigoni, C. Russo, R. Cancedda, A. Pagano, Selection of candidate housekeeping genes for normalization in human postmortem brain samples., Int. J. Mol. Sci. 12 (2011) 5461–70. doi:10.3390/ijms12095461.

[122] M. Intrieri, A. Rinaldi, O. Scudiero, G. Autiero, G. Castaldo, G. Nardone, Low expression of human β-defensin 1 in duodenum of celiac patients is partially restored by a gluten-free diet, Clin. Chem. Lab. Med. 48 (2010) 489–92. doi:10.1515/CCLM.2010.098.

[123] K.J. Livak, T.D. Schmittgen, Analysis of relative gene expression data using real-time quantitative PCR and the 2(-Delta Delta C(T)) Method., Methods. 25 (2001) 402–8. doi:10.1006/meth.2001.1262.

[124] W.A.W. Ruzali, P.G. Kehoe, S. Love, LRP1 expression in cerebral cortex, choroid plexus and meningeal blood vessels: Relationship to cerebral amyloid angiopathy and APOE status, Neurosci. Lett. 525 (2012) 123–128. doi:10.1016/j.neulet.2012.07.065.

[125] R.S. Doody, R. Raman, R.A. Sperling, E. Seimers, G. Sethuraman, R. Mohs, M. Farlow, T. Iwatsubo, B. Vellas, X. Sun, K. Ernstrom, R.G. Thomas, P.S. Aisen, Peripheral and central effects of γ-secretase inhibition by semagacestat in Alzheimer's disease, Alzheimers. Res. Ther. 7 (2015) 36. doi:10.1186/s13195-015-0121-6.

[126] V. Coric, S. Salloway, C.H. van Dyck, B. Dubois, N. Andreasen, M. Brody, C. Curtis, H. Soininen, S. Thein, T. Shiovitz, G. Pilcher, S. Ferris, S. Colby, W. Kerselaers, R. Dockens, H. Soares, S. Kaplita, F. Luo, C. Pachai, L. Bracoud, M. Mintun, J.D. Grill, K. Marek, J. Seibyl, J.M. Cedarbaum, C. Albright, H.H. Feldman, R.M. Berman, Targeting Prodromal Alzheimer Disease With Avagacestat: A Randomized Clinical Trial., JAMA Neurol. 72 (2015) 1324–33. doi:10.1001/jamaneurol.2015.0607.

[127] N.K. LoConte, A.R.A. Razak, P. Ivy, A. Tevaarwerk, R. Leverence, J. Kolesar, L. Siu, S.J. Lubner, D.L. Mulkerin, W.R. Schelman, D.A. Deming, K.D. Holen, L. Carmichael, J. Eickhoff,

G. Liu, A multicenter phase 1 study of γ -secretase inhibitor RO4929097 in combination with capecitabine in refractory solid tumors, Invest. New Drugs. 33 (2015) 169–176. doi:10.1007/s10637-014-0166-6.

[128] R. Penninkilampi, H.M. Brothers, G.D. Eslick, Pharmacological Agents Targeting γ-Secretase Increase Risk of Cancer and Cognitive Decline in Alzheimer's Disease Patients: A Systematic Review and Meta-Analysis, J. Alzheimer's Dis. JAD. 53 (2016) 1395–1404. doi:10.3233/JAD-160275.

[129] X. Cao, T.C. Südhof, Dissection of amyloid-beta precursor protein-dependent transcriptional transactivation, J. Biol. Chem. 279 (2004) 24601–24611. doi:10.1074/jbc.M402248200.

[130] M.R. Hass, B.A. Yankner, A {gamma}-secretase-independent mechanism of signal transduction by the amyloid precursor protein, J. Biol. Chem. 280 (2005) 36895–36904. doi:10.1074/jbc.M502861200.

[131] S. Xu, R. Wilf, T. Menon, P. Panikker, J. Sarthi, F. Elefant, Epigenetic control of learning and memory in Drosophila by Tip60 HAT action, Genetics. 198 (2014) 1571–1586. doi:10.1534/genetics.114.171660.

[132] A. Kinoshita, C.M. Whelan, O. Berezovska, B.T. Hyman, The γ Secretase-generated Carboxyl-terminal Domain of the Amyloid Precursor Protein Induces Apoptosis via Tip60 in H4 Cells, J. Biol. Chem. 277 (2002) 28530–28536. doi:10.1074/jbc.M203372200.

[133] C. Broder, C. Becker-Pauly, The metalloproteases meprin α and meprin β: unique enzymes in inflammation, neurodegeneration, cancer and fibrosis, Biochem. J. 450 (2013) 253–264. doi:10.1042/BJ20121751.

[134] M. Brkic, S. Balusu, E. Van Wonterghem, N. Gorlé, I. Benilova, A. Kremer, I. Van Hove, L. Moons, B. De Strooper, S. Kanazir, C. Libert, R.E. Vandenbroucke, Amyloid β Oligomers Disrupt Blood-CSF Barrier Integrity by Activating Matrix Metalloproteinases., J. Neurosci. 35 (2015) 12766–78. doi:10.1523/JNEUROSCI.0006-15.2015.

[135] M. Brkic, S. Balusu, C. Libert, R.E. Vandenbroucke, Friends or Foes: Matrix Metalloproteinases and Their Multifaceted Roles in Neurodegenerative Diseases, Mediators Inflamm. 2015 (2015) 620581. doi:10.1155/2015/620581.

[136] T.L. Tekirian, Commentary: Abeta N- Terminal Isoforms: Critical contributors in the course of AD pathophysiology., J. Alzheimers. Dis. 3 (2001) 241–248. http://www.ncbi.nlm.nih.gov/pubmed/12214065.

[137] C. Becker-Pauly, C.U. Pietrzik, The Metalloprotease Meprin β Is an Alternative β-Secretase of APP, Front. Mol. Neurosci. 9 (2016) 159. doi:10.3389/fnmol.2016.00159.

[138] R.F. Miguel, A. Pollak, G. Lubec, Metalloproteinase ADAMTS-1 but not ADAMTS-5 is manifold overexpressed in neurodegenerative disorders as Down syndrome, Alzheimer's and Pick's disease, Mol. Brain Res. 133 (2005) 1–5. doi:10.1016/j.molbrainres.2004.09.008.

[139] M.A. Bruno, E.J. Mufson, J. Wuu, A.C. Cuello, Increased matrix metalloproteinase 9 activity in mild cognitive impairment, J. Neuropathol. Exp. Neurol. 68 (2009) 1309–1318. doi:10.1097/NEN.0b013e3181c22569.

[140] J. Bien, T. Jefferson, M. Causević, T. Jumpertz, L. Munter, G. Multhaup, S. Weggen, C.

Becker-Pauly, C.U. Pietrzik, The metalloprotease meprin β generates amino terminal-truncated amyloid β peptide species, J. Biol. Chem. 287 (2012) 33304–33313. doi:10.1074/jbc.M112.395608.

[141] D. Lottaz, C.A. Maurer, A. Noël, S. Blacher, M. Huguenin, A. Nievergelt, V. Niggli, A. Kern, S. Müller, F. Seibold, H. Friess, C. Becker-Pauly, W. Stöcker, E.E. Sterchi, Enhanced activity of meprin-α, a pro-migratory and pro-angiogenic protease, in colorectal cancer, PLoS One. 6 (2011) e26450. doi:10.1371/journal.pone.0026450.

[142] C. Schönherr, J. Bien, S. Isbert, R. Wichert, J. Prox, H. Altmeppen, S. Kumar, J. Walter, S.F. Lichtenthaler, S. Weggen, M. Glatzel, C. Becker-Pauly, C.U. Pietrzik, Generation of aggregation prone N-terminally truncated amyloid β peptides by meprin β depends on the sequence specificity at the cleavage site., Mol. Neurodegener. 11 (2016) 19. doi:10.1186/s13024-016-0084-5.

[143] T. Jefferson, M. Čaušević, U. Auf dem Keller, O. Schilling, S. Isbert, R. Geyer, W. Maier, S. Tschickardt, T. Jumpertz, S. Weggen, J.S. Bond, C.M. Overall, C.U. Pietrzik, C. Becker-Pauly, Metalloprotease meprin beta generates nontoxic N-terminal amyloid precursor protein fragments in vivo, J. Biol. Chem. 286 (2011) 27741–27750. doi:10.1074/jbc.M111.252718.

[144] B.M. Austen, D.J. Stephens, Cleavage of a beta-amyloid precursor sequence by cathepsin D., Biomed. Pept. Proteins Nucleic Acids. 1 (1995) 243–6. http://www.ncbi.nlm.nih.gov/pubmed/9346839.

[145] U. Haas, D.L. Sparks, Cortical cathepsin D activity and immunolocalization in Alzheimer disease, critical coronary artery disease, and aging., Mol. Chem. Neuropathol. 29 (1996) 1–14. doi:10.1007/BF02815189.

[146] T. Kobayashi, K. Honke, S. Gasa, T. Fujii, S. Maguchi, T. Miyazaki, A. Makita, Proteolytic processing sites producing the mature form of human cathepsin D., Int. J. Biochem. 24 (1992) 1487–91. http://www.ncbi.nlm.nih.gov/pubmed/1426530.

[147] F. Letronne, G. Laumet, A.-M. Ayral, J. Chapuis, F. Demiautte, M. Laga, M.E. Vandenberghe, N. Malmanche, F. Leroux, F. Eysert, Y. Sottejeau, L. Chami, A. Flaig, C. Bauer, P. Dourlen, M. Lesaffre, C. Delay, L. Huot, J. Dumont, E. Werkmeister, F. Lafont, T. Mendes, F. Hansmannel, B. Dermaut, B. Deprez, A.-S. Hérard, M. Dhenain, N. Souedet, F. Pasquier, D. Tulasne, C. Berr, J.-J. Hauw, Y. Lemoine, P. Amouyel, D. Mann, R. Déprez, F. Checler, D. Hot, T. Delzescaux, K. Gevaert, J.-C. Lambert, ADAM30 Downregulates APP-Linked Defects Through Cathepsin D Activation in Alzheimer's Disease., EBioMedicine. 9 (2016) 278–292. doi:10.1016/j.ebiom.2016.06.002.

[148] E. Karran, B. De Strooper, The amyloid cascade hypothesis: are we poised for success or failure?, J. Neurochem. 139 (2016) 237–252. doi:10.1111/jnc.13632.

[149] W. Wang, A.M. Moerman-Herzog, A. Slaton, S.W. Barger, Presenilin 1 mutations influence processing and trafficking of the ApoE receptor apoER2, Neurobiol. Aging. 49 (2017) 145–153. doi:10.1016/j.neurobiolaging.2016.10.005.

[150] J.A. Larios, I. Jausoro, M.-L. Benitez, F.C. Bronfman, M.-P. Marzolo, Neurotrophins regulate ApoER2 proteolysis through activation of the Trk signaling pathway, BMC Neurosci. 15 (2014) 108. doi:10.1186/1471-2202-15-108.

[151] I. Cuchillo-Ibañez, T. Mata-Balaguer, V. Balmaceda, J.J. Arranz, J. Nimpf, J. Sáez-Valero, The β-amyloid peptide compromises Reelin signaling in Alzheimer's disease., Sci. Rep. 6 (2016)

31646. doi:10.1038/srep31646.

[152] A. Sogorb-Esteve, M.-S. García-Ayllón, M. Llansola, V. Felipo, K. Blennow, J. Sáez-Valero, Inhibition of γ-Secretase Leads to an Increase in Presenilin-1., Mol. Neurobiol. (2017). doi:10.1007/s12035-017-0705-1.

[153] H. Acx, L. Serneels, E. Radaelli, S. Muyldermans, C. Vincke, E. Pepermans, U. Müller, L. Chávez-Gutiérrez, B. De Strooper, Inactivation of γ-secretases leads to accumulation of substrates and non-Alzheimer neurodegeneration, EMBO Mol. Med. 9 (2017) 1088–1099. doi:10.15252/emmm.201707561.

[154] L.B. Gatta, A. Albertini, R. Ravid, D. Finazzi, Levels of beta-secretase BACE and alpha-secretase ADAM10 mRNAs in Alzheimer hippocampus., Neuroreport. 13 (2002) 2031–3. http://www.ncbi.nlm.nih.gov/pubmed/12438920.